

International Atomic Energy Agency

INDC(CCP)-298/L

---

**INDC**

---

---

**INTERNATIONAL NUCLEAR DATA COMMITTEE**

---

TRANSLATION OF SELECTED PAPERS  
PUBLISHED IN NUCLEAR CONSTANTS 2, 1988

(Original Report in Russian was distributed  
as INDC(CCP)-294/G)

Translated by the IAEA

April 1989

---

**IAEA NUCLEAR DATA SECTION, WAGRAMERSTRASSE 5, A-1400 VIENNA**

TRANSLATION OF SELECTED PAPERS  
PUBLISHED IN NUCLEAR CONSTANTS 2, 1988

(Original Report in Russian was distributed  
as INDC(CCP)-294/G)

Translated by the IAEA

April 1989

Reproduced by the IAEA in Austria  
April 1989

89-01353

## Contents

### Calculation of Integral Delayed Neutron Properties

#### Part 1: Total Neutron Yield

L.G. Manevich, P.Eh. Nemirovskij, M.S. Yudkevich ..... 5

### Calculation of Integral Delayed Neutron Properties

#### Part 2: Group Constants and Reactivity

L.G. Manevich, P.Eh. Nemirovskij, M.S. Yudkevich ..... 21

### Uranium and Plutonium Energy Release per Fission Event in a Nuclear Reactor

A.F. Badalov, V.I. Kopejkin ..... 37

### The Use of Evaluated Nuclear Data Libraries for the Calculation of Kerma Factors

I.M. Bondarenko, A.S. Zabrodskaya, A.S. Krivtsov,  
I.N. Nikolaev ..... 47

### Target Properties and Nuclear Data

N.V. Kornilov, A.A. Goverdovskij ..... 53

### Cross-Sections for the Production of $\gamma$ -Rays by the Interaction of 3.0 MeV Neutrons with $^{232}\text{Th}$ , $^{235}\text{U}$ and $^{238}\text{U}$ Nuclei

A.A. Filatenkov, M.V. Blinov, S.V. Chubaev,  
V.M. Saidgareev ..... 63

## CALCULATION OF INTEGRAL DELAYED NEUTRON PROPERTIES

### Part 1. Total neutron yield

L.G. Manevich, P.Eh. Nemirovskij, M.S. Yudkevich

CALCULATION OF INTEGRAL DELAYED NEUTRON PROPERTIES. PART 1. TOTAL DELAYED NEUTRON YIELD. The total delayed neutron yield was derived from nuclear data and the fission yields of the individual precursors. Agreement with experimental measurements is acceptable for the cases of 25 fissionable nuclides.

In current analyses of reactor kinetics use is made of data on the properties of delayed neutrons derived from the results of macroscopic experiments. By now, fairly full information has been accumulated on fission fragments emitting delayed neutrons. The nuclei which have not been investigated represent only a small contribution, which can be evaluated on the basis of theoretical considerations and systematics. This makes it possible to determine the integral properties of delayed neutrons as the sum of the contributions of individual nuclei thereto. It is not impossible that this microscopic approach will ensure greater accuracy than the traditional macroscopic one.

The present paper comprises calculation of the total delayed neutron fission yield  $\nu_d$ . This quantity has been measured with an accuracy of 5-10% for practically all fissionable nuclei at various energies of the neutrons causing fission. A comparison of the calculated and measured values for  $\nu_d$  gives an indication of the reliability of the data used for the calculations and of the assumptions made. In cases of good agreement, these data may also be used for calculating other integral properties of delayed neutrons.

The value of  $\nu_d$  was derived for thermal neutron fission of  $^{233,235}\text{U}$  and  $^{239,241}\text{Pu}$ , and fission of  $^{232}\text{Th}$ ,  $^{235,238}\text{U}$  and  $^{239}\text{Pu}$  by the fissioning spectrum; it was obtained with somewhat inferior accuracy for the fast neutron fission of  $^{233,236}\text{U}$ ,  $^{237}\text{Np}$  and  $^{240,241,242}\text{Pu}$ , and 14 MeV neutron fission of  $^{232}\text{Th}$ ,  $^{233,235,238}\text{U}$  and  $^{239}\text{Pu}$ . Evaluational calculations of  $\nu_d$  were carried

out for the exotic nuclei  $^{229}\text{Th}$ ,  $^{238}\text{Pu}$ ,  $^{241}\text{Am}$  and  $^{243,244,245,247,247}\text{Cm}$ .

Calculation of the yield  $\nu_d$  has indeed been carried out before [1-4], but the values obtained in the works in question are strongly at variance with the measurement results even for the most thoroughly investigated fissionable isotopes. Calculation of  $\nu_d$  amounts to evaluating the probability of neutron emission during the decay of the fission-fragment nuclei  $P_n$  and the cumulative fragment yield  $q$ . The present paper gives the evaluated values for  $P_n$  in respect of 111 nuclides and their yield  $q$  upon fission of the host fissionable nuclides.

#### Evaluation of the delayed neutron fraction per nuclide disintegration.

All delayed neutron emitters can be divided into two groups: experimentally investigated fragments, for which the probability of disintegration with neutron emission  $P_n$  has been determined, and uninvestigated fragments, for whose evaluation recourse must be had to systematics.

In 1977, G. Rudstam published a compendium of experimental data [5] on the probability  $P_n$  for 45 nuclei. Later the same investigator published another review, this time for 65 fragments [6]. Supplementary information is contained in Refs [7-9].

Thus, in Ref. [6] data are quoted on the probability  $P_n$  for 65 emitters, although the unreliability of the results derived for the nuclides  $^{97,98}\text{Y}$  and  $^{97,98}\text{Sr}$  and also for barium and lanthanum is to be noted. According to our evaluations,  $^{147}\text{Ba}$  should not emit delayed neutrons at all. More recently, data [9] have been published which contest the results of study [6] for the above nuclides. According to Ref. [9], the contribution of barium and lanthanum is so small as to be negligible. This view has indeed been adopted in the present work. Our proposals on the  $P_n$  for strontium and yttrium diverge only slightly from the data in Ref. [9]. Thus, the group of known emitter nuclides contains 59 nuclei [6], to which should be added two further nuclei from Ref. [9].

Table 1. Values of  $P_n$  for investigated emitters, %.

Nuclide	Data from			Nuclide	Data from		
	the present work	/10/	/11/		the present work	/10/	/11/
<sup>79</sup> Ga	0,098±0,01	0,098±0,01	0,100	<sup>99</sup> Y	1,2±0,8	1,2±0,8	1,3
<sup>80</sup> Ga	0,84±0,06	0,084±0,06	0,86	<sup>127m</sup> In	0,68±0,2	0,68±0,06	0,69
<sup>81</sup> Ga	12±0,9	12±0,9	12,2	<sup>127g</sup> In	0,04±0,04	—	—
<sup>82</sup> Ga	21,4±2,2	21,4±2,2	21,6	<sup>128</sup> In	0,059±0,008	0,059	0,060
<sup>83</sup> Ga	43±7	43±7	43,9	<sup>129m</sup> In	2,5±0,5	2,5±0,5	3,0
<sup>84</sup> As	0,13±0,05	0,09±0,05	0,078	<sup>129g</sup> In	0,25	0,25±0,05	0,25
<sup>85</sup> As	22,7±8	53±18	22	<sup>130</sup> In	1,40±0,09	1,4±0,09	1,39
<sup>86</sup> As	6,2±3	12±3	10,5	<sup>131</sup> In	1,72±0,23	1,72±0,23	1,61
<sup>87</sup> As	44±15	44	44	<sup>132</sup> In	4,2±0,9	4,2±0,9	4,1
<sup>87</sup> Se	0,18±0,03	0,19±0,03	0,18	<sup>134</sup> Sn	17±7	17±7	18
<sup>88</sup> Se	0,15	0,6±0,3	0,96	<sup>134</sup> Sb	0,114±0,006	0,112±0,009	0,117
<sup>89</sup> Se	4±1,0	5±1,5	7,5	<sup>135</sup> Sb	15,5±1,0	16,4±1,8	20,8
<sup>91</sup> Se	21±8	21±8	21	<sup>136</sup> Sb	23±7	23±8	23
<sup>87</sup> Br	2,512±0,15	2,48±0,11	2,58	<sup>136</sup> Te	0,9±0,3	0,9±0,4	1,14
<sup>88</sup> Br	6,817±0,3	6,6±0,3	6,35	<sup>137</sup> Te	2,2±0,5	2,5±0,5	2,7
<sup>89</sup> Br	13,6±0,9	14,0±0,7	14,2	<sup>138</sup> Te	5,6±2,0	6,3±2,1	6,7
<sup>90</sup> Br	23,4±1,5	23,5±1,4	24,9	<sup>137</sup> I	6,4±0,3	6,5±0,3	7,1
<sup>91</sup> Br	15,2±4	19,2±1,3	18,3	<sup>138</sup> I	5,1±0,5	5,3±0,4	5,5
<sup>92</sup> Br	20,0±7	22±6	—	<sup>139</sup> I	9,7±0,6	9,8±0,5	9,9
<sup>92</sup> Kr	0,033±0,033	0,033±0,003	0,031	<sup>140</sup> I	9,3±0,6	9,2±0,5	9,4
<sup>93</sup> Kr	1,9±0,14	1,96±0,14	1,93	<sup>141</sup> I	22,1±3	21,2±3	21,7
<sup>94</sup> Kr	2,2±1,0	5,7±2,2	6,1	<sup>141</sup> Xe	0,043±0,005	0,044±0,005	0,041
<sup>92</sup> Rb	0,012±0,001	0,0108±0,0007	0,0100	<sup>142</sup> Xe	0,406±0,04	0,42±0,04	0,39
<sup>93</sup> Rb	1,44±0,06	1,31±0,06	1,36	<sup>141</sup> Cs	0,036±0,002	0,029±0,002	0,034
<sup>94</sup> Rb	10,4±0,6	9,9±0,3	10,2	<sup>142</sup> Cs	0,099±0,005	0,093±0,006	0,096
<sup>95</sup> Rb	8,8±0,5	8,5±0,3	8,6	<sup>143</sup> Cs	1,69±0,1	1,61±0,08	1,63
<sup>96</sup> Rb	14,4±0,7	13,3±0,5	14,2	<sup>144</sup> Cs	2,86±0,2	3,1±0,3	3,17
<sup>97</sup> Rb	29±6	25,1±1,3	26,9	<sup>145</sup> Cs	14,3±1,0	13,6±1,0	13,4
<sup>98</sup> Rb	15±1	15,1±1,2	13,4	<sup>146</sup> Cs	13,4±0,8	13,3±0,6	13,4
<sup>99</sup> Rb	13,4±3	15±3	13,4	<sup>147</sup> Cs	25,4±3,2	25,4±3,2	26,2
<sup>99</sup> Sr	2,5±2	3,4	3,6				

Using the data of the works mentioned above, an evaluation was made of the probability of  $P_n$  for various nuclides. In respect of emitters for which a number of measurements exist, averaging was carried out with weighting for the inversely proportional square of the error. Where the measurements did not agree within the limits of the errors stated, preference was given to the more recent data. The results of evaluation of  $P_n$  are given in Table 1. Apart from these data, reference may be made to study [12], where  $P_n$  values are quoted for 97 nuclei (for 41 nuclei the evaluation is performed on the basis of theoretical considerations).

There is on the whole agreement between the various evaluations. There is a strong discrepancy only for the evaluation of <sup>85</sup>As; in Ref. [6] a  $P_n$

of  $(53 \pm 18)\%$  is given. Such a large percentage of disintegrations into a continuous spectrum for  $^{85}\text{As}$  is unlikely from a theoretical point of view, since the neutron binding energy in the daughter nucleus  $^{85}\text{Se}$  is 4.75 MeV and the number of discrete levels in this range is large. The value  $P_n = 53\%$  contradicts the measurements in Ref. [13], which obtains  $P_n = (22 \pm 8)\%$ . We consider that the values given in Ref. [6] for  $^{85}\text{As}$  are incorrect.

Alongside the "investigated" delayed neutron emitters there exists a large number which have not been investigated. Reference [3] studied 248 such emitters with  $25 \leq Z \leq 61$ . The majority of them have an insignificant yield, but about 50 nuclides may make a contribution to the determination of  $\nu_d$ .

Emission of delayed neutrons occurs if the  $\beta$ -decay energy of the parent nucleus is greater than the binding energy of the neutron in the daughter nucleus, i.e. if  $E_\beta(Z, A) > E_n(Z + 1, A)$ . Here,  $\beta$ -decay may occur in the continuous spectrum state of the daughter nucleus with subsequent emission of delayed neutrons. Energies  $E_\beta$  and  $E_n$  can be evaluated using the data of Ref. [14], to within 0.5 MeV or somewhat better.

For gallium, arsenic, selenium, bromine, rubidium, iodine and other nuclides with known delayed neutron emitters, the difference  $E_\beta - E_n$  is greater than zero for nuclides with a number of nucleons  $N_0$  such that, when  $N < N_0$ , the quantity  $P_n = 0$ , and when  $N \geq N_0$ , the value  $P_n > 0$  is in agreement with experiment. From our evaluations of the energy difference  $E_\beta - E_n$  for germanium, strontium, yttrium, zirconium, niobium, molybdenum, technetium, barium and lanthanum, it follows that they are delayed neutron emitters.

For evaluating the probability  $P_n$  use is normally made of formula [15]

$$P_n = C \left( \frac{E_\beta - E_n}{E_\beta - b} \right)^{4.35}, \quad (1)$$

where  $C$  is a constant equal to 125;  $b$  is a constant equal to 0 at  $N_{\text{even}}$ ,  $Z_{\text{even}}$ ,  $b = 13/A^{1/2}$  for  $A_{\text{odd}}$ ,  $b = 26/A^{1/2}$  for  $N_{\text{odd}}$ ,  $Z_{\text{odd}}$ . Expression (1) has



no firm theoretical foundation and for nuclei with known  $P_n$  does not give a satisfactory result. We therefore considered the minimum and maximum evaluations of  $P_n$  following from expression (1) on the basis of two propositions:

1. Upon the disintegration of nuclei with  $Z_{\text{even}}$  the value of  $P_n$  is an order of magnitude less than in the case of nuclei with  $Z_{\text{odd}}$  at the same  $Z/A$  relationship;
2. In nuclei with ground state  $(9/2)^+$  (nuclides of niobium and technetium), disintegration with emission of delayed neutrons is rendered difficult, since there are in the continuous spectrum of the daughter nucleus few levels with substantial spin owing to the strong centrifugal barrier.

Table 2 shows the evaluations obtained and their comparison with the data from study [3]. It should be pointed out that in this latter study the calculations were, in our opinion, conducted with unreliable experimental values of  $P_n$  for  $^{97,98}\text{Sr}$ ,  $^{98}\text{Y}$  and  $^{147,148}\text{Ba}$ . In fact, new data have made it possible to derive [9, 16] other values of  $P_n$  for the above-mentioned nuclides (and in particular to dispense with the very high  $P_n$  values  $^{98}\text{Y}$  and  $^{147,148}\text{Ba}$ ). Reference [9] cites the following values of  $P_n$ , %:  $^{98}\text{Sr} - 0.18$ ,  $^{98}\text{Y} - 0.23$ ,  $^{99}\text{Sr} - 0.31$ ,  $^{99}\text{Y} - 0.96$  and  $^{147,148}\text{Ba} - 0.03$ .

In all the following calculations use was made of the minimum evaluation from Table 2. Agreements of the yield  $v_d$  with experiment emerges here as satisfactory. Allowance for the data in Ref. [17] for strontium and yttrium may result in some reduction of the yield  $v_d$ .

Yield of emitters upon fission. The cumulative yield  $q$  of delayed neutron emitter fragments is known with good accuracy in respect of thermal neutron fission of  $^{235}\text{U}$ ,  $^{239}\text{Pu}$  and  $^{233}\text{U}$  (mainly for fragments with  $T_{1/2} > 1$  s) involving substantial yield. Fairly accurate data for fission spectrum neutron fission are available for  $^{232}\text{Th}$ ,  $^{235}\text{U}$  and  $^{238}\text{U}$ .

Table 2. Evaluations of  $P_n$  for uninvestigated emitters, %.

Nuclide	Data from			Nuclide	Data from		
	Min. eval. from present study	$\sqrt{A}$	Max. eval. from present study		Min. eval. from present study	$\sqrt{A}$	Max. eval. from present study
$^{79}\text{Zn}$	1,0	1,1	2,0	$^{103}\text{Nb}$	0,13	0,13	0,2
$^{83}\text{Ge}$	0,1	0,17	0,4	$^{104}\text{Nb}$	0,56	0,71	1,0
$^{84}\text{Ge}$	5	10	5	$^{105}\text{Nb}$	1,7	2,9	3,5
$^{85}\text{Ge}$	10	20	25	$^{106}\text{Nb}$	3,5	5,5	8,0
$^{86}\text{Ge}$	15	22	30	$^{107}\text{Nb}$	10	-	20
$^{88}\text{As}$	10	-	30	$^{109}\text{Mo}$	0	0,53	0
$^{89}\text{As}$	30	-	50	$^{110}\text{Mo}$	0,1	1,3	1,0
$^{90}\text{Se}$	5	11	15	$^{111}\text{Mo}$	0,5	-	3,0
$^{93}\text{Br}$	25	41	25	$^{109}\text{Tc}$	0,5	1,7	2,3
$^{94}\text{Br}$	40	-	50	$^{110}\text{Tc}$	10	3,1	20
$^{95}\text{Kr}$	7	9,5	12	$^{111}\text{Tc}$	15	-	20
$^{96}\text{Kr}$	15	-	30	$^{112}\text{Tc}$	20	-	30
$^{97}\text{Sr}$	0,2	0,27	0,3	$^{128}\text{Cd}$	0,1	0,1	0,2
$^{98}\text{Sr}$	0,3	0,36	1,0	$^{133}\text{Sn}$	0,02	0,02	0,03
$^{100}\text{Sr}$	3	5,6	10	$^{135}\text{Sn}$	8,6	8,6	25
$^{101}\text{Sr}$	10	-	15	$^{137}\text{Sb}$	15	20	30
$^{97}\text{Y}$	0,06	0,33	1,6	$^{139}\text{Te}$	6	6,3	10
$^{98}\text{Y}$	0,7	0,54	1,0	$^{140}\text{Te}$	15	-	20
$^{100}\text{Y}$	2	5,5	5,5	$^{142}\text{I}$	20	16	40
$^{101}\text{Y}$	1,1	-	6	$^{143}\text{I}$	25	18	45
$^{102}\text{Y}$	4	-	15	$^{143}\text{Xe}$	1,2	1,2	2,0
$^{103}\text{Y}$	15	-	30	$^{144}\text{Xe}$	2	0,73	2,5
$^{104}\text{Y}$	20	-	50	$^{147}\text{Ba}$	0	5,2	0
$^{104}\text{Zr}$	0	0,11	0	$^{148}\text{Ba}$	0,2	23,9	0,5
$^{105}\text{Zr}$	0,05	1,4	1,0	$^{147}\text{La}$	0,1	5	0,5

Fission data for other nuclei are limited, and hence it is necessary to have recourse to evaluations based on accurately measured fragment mass distributions. From a known mass distribution, the charge distribution for a specific mass is derived on the basis of the following considerations:

1. Charge distribution for a particular value of  $A$  is Gaussian, i.e.

$$f(Z) = a \exp \left[ -(Z - Z_0)^2 / b^2 \right], \quad (2)$$

where  $a$  is a normalizing constant;  $b$  is determined from experimental data (on  $^{235}\text{U}$  for all nuclides except  $^{238}\text{U}$  and  $^{232}\text{Th}$ , for which this constant is determined from  $^{238}\text{U}$ );

2. The most likely charge  $Z_0$  for a given value of  $A$  is determined for a light fragment by the formula

$$Z_0^L = Z_f \frac{A_L}{A_f - (v-1)} + \alpha, \quad (3)$$

where  $Z_f$ ,  $A_f$  are the charge and mass number of the target nucleus;  $\nu$  is the number of secondary fission neutrons; and  $\alpha$  is the displacement constant (for thermal neutron fission  $\alpha \sim 0.5$ ). For a heavy fragment the charge  $Z_o^h = Z_f - Z_o^l$ ;

3. It is known from experiment that upon fission of  $^{233,235,238}\text{U}$  the yield of fragments with even  $Z$  is somewhat greater (about 15-20%) compared with the yield ensuing from formula (2), and the yield with odd  $Z$  is attenuated. For thorium and plutonium this effect is less pronounced.

Thus, we have modified somewhat the fragment distribution obtained in study [17], in accordance with currently available experimental data. In addition, for  $^{232}\text{Th}$  and  $^{238}\text{U}$  the fragment distribution is broadened in order to secure agreement with the experimental value for the yield  $\nu_d$ , since here there was an increased content of nuclides with high neutron excess, which has not been adequately determined experimentally. In the case of thermal neutron fission of  $^{229}\text{Th}$  and  $^{243,245,247}\text{Cm}$  and in that of fast neutron fission of  $^{241}\text{Am}$ , for which there are no data in study [17], fragment fission was calculated on the basis of formulae (2)-(4).

Using the derived probabilities  $P_n$  and the yield  $q_z$ , we obtained the cumulative yield which is defined as the sum of the individual yield from a given emitter upon fission and the yield of all its  $\beta$ -precursors less  $\beta$ -disintegrations with emission of delayed neutrons:

$$q = \sum_{Z < Z_i} q_{Z_i} (1 - P_i) + q_{Z_i} \quad (4)$$

Calculation of the cumulative yield has been performed for all fissionable nuclides (see below). In Table 3 we give the cumulative yield of fragments contributing to the quantity  $\nu_d$  upon fission of thermal reactor host nuclides.

Data on 14 MeV neutron fission are not quoted. The approximate doubling of the number  $\nu$  (from 2.5 to 4.5) means that the  $^{235}\text{U}$  fragment

**Table 3.** Cumulative yield of emitters per fission and error associated with yield upon thermal neutron fission of  $^{235}\text{U}$ , and  $^{239}$ ,  $^{241}\text{Pu}$  and fast neutron fission of  $^{238}\text{U}$ , %.

Nuclide	$^{235}\text{U}$		$^{238}\text{U}$		$^{239}\text{Pu}$		$^{241}\text{Pu}$	
	q	$\Delta q$	q	$\Delta q$	q	$\Delta q$	q	$\Delta q$
$^{79}\text{Ga}$	$1,8 \cdot 10^{-2}$	20	$2,2 \cdot 10^{-2}$	20	$5,8 \cdot 10^{-3}$	20	$6 \cdot 10^{-3}$	40
$^{80}\text{Ga}$	$1,2 \cdot 10^{-2}$	20	$2,5 \cdot 10^{-2}$	20	$8,8 \cdot 10^{-3}$	30	$5 \cdot 10^{-3}$	40
$^{81}\text{Ga}$	$7,6 \cdot 10^{-3}$	30	$2,4 \cdot 10^{-2}$	20	$3,3 \cdot 10^{-3}$	40	$3 \cdot 10^{-3}$	50
$^{82}\text{Ga}$	$4,6 \cdot 10^{-3}$	40	$1,3 \cdot 10^{-2}$	30	-	-	$1,1 \cdot 10^{-3}$	50
$^{84}\text{Ge}$	$2,1 \cdot 10^{-2}$	30	0,125	20	$3 \cdot 10^{-3}$	30	$1,2 \cdot 10^{-2}$	50
$^{85}\text{Ge}$	$4 \cdot 10^{-3}$	40	0,031	50	-	-	$3 \cdot 10^{-3}$	50
$^{84}\text{As}$	$2,7 \cdot 10^{-1}$	5	0,556	10	0,1	10	0,13	30
$^{85}\text{As}$	0,156	5	0,302	40	$2,35 \cdot 10^{-2}$	10	$0,6 \cdot 10^{-2}$	30
$^{86}\text{As}$	$8,6 \cdot 10^{-2}$	10	0,25	50	$1,13 \cdot 10^{-2}$	10	$3,2 \cdot 10^{-2}$	30
$^{87}\text{As}$	$4,5 \cdot 10^{-2}$	30	0,111	50	$1,9 \cdot 10^{-3}$	50	$7 \cdot 10^{-2}$	30
$^{88}\text{As}$	$2,4 \cdot 10^{-2}$	50	$4 \cdot 10^{-2}$	50	-	-	$1 \cdot 10^{-3}$	50
$^{87}\text{Se}$	0,79	5	1,1	10	0,145	10	0,294	10
$^{88}\text{Se}$	0,435	15	0,907	10	$5,2 \cdot 10^{-2}$	10	0,125	20
$^{89}\text{Se}$	0,1	10	0,565	30	$6,5 \cdot 10^{-3}$	10	$3,6 \cdot 10^{-2}$	30
$^{90}\text{Se}$	$1 \cdot 10^{-2}$	30	0,175	50	-	-	$1,2 \cdot 10^{-2}$	50
$^{87}\text{Br}$	2,044	2	1,515	4	0,7	6	0,622	4
$^{88}\text{Br}$	1,913	6	1,88	25	0,532	6	0,593	8
$^{89}\text{Br}$	1,4	2,8	2,09	25	0,351	6	0,419	16
$^{90}\text{Br}$	0,62	8	1,48	30	0,105	8	0,25	8
$^{91}\text{Br}$	0,227	10	0,886	30	$1,71 \cdot 10^{-2}$	20	$9,2 \cdot 10^{-2}$	20
$^{92}\text{Br}$	$3,5 \cdot 10^{-2}$	15	0,302	50	$1,85 \cdot 10^{-2}$	20	$2,85 \cdot 10^{-2}$	30
$^{93}\text{Br}$	-	-	$7,7 \cdot 10^{-2}$	50	-	-	$4,8 \cdot 10^{-3}$	50
$^{92}\text{Kr}$	1,9	8,5	3,14	10	0,30	5	0,91	30
$^{93}\text{Kr}$	0,584	10	1,99	15	0,07	10	0,421	30
$^{94}\text{Kr}$	0,155	30	0,754	25	0,02	30	0,114	30
$^{92}\text{Rb}$	4,91	3	4,43	10	2,00	5	2,05	5
$^{93}\text{Rb}$	3,86	2	4,465	11	1,823	16	1,892	25
$^{94}\text{Rb}$	1,86	3	3,37	30	0,808	16	1,304	25
$^{95}\text{Rb}$	0,63	3	2,052	23	0,24	20	0,658	35
$^{96}\text{Rb}$	0,18	15	0,93	40	$4,7 \cdot 10^{-2}$	30	0,2	30
$^{97}\text{Rb}$	$7,8 \cdot 10^{-2}$	10	0,242	50	$6,2 \cdot 10^{-3}$	30	$4,4 \cdot 10^{-2}$	50
$^{98}\text{Rb}$	$3 \cdot 10^{-3}$	50	$4,7 \cdot 10^{-2}$	50	-	-	$6,6 \cdot 10^{-3}$	50
$^{97}\text{Sr}$	1,97	5	3,35	5	0,75	10	1,8	10
$^{98}\text{Sr}$	0,85	10	1,78	5	0,233	20	0,667	30
$^{99}\text{Sr}$	0,35	10	0,66	10	$3,6 \cdot 10^{-2}$	20	0,18	30
$^{100}\text{Sr}$	0,067	30	0,125	20	$7 \cdot 10^{-3}$	50	$5,3 \cdot 10^{-2}$	50
$^{97}\text{Y}$	5,3	3	5,28	4	3,83	3	4,16	5
$^{98}\text{Y}$	2,99	10	4,85	4	2,27	5	3,14	10
$^{99}\text{Y}$	2,43	5	3,7	4	1,2	5	2,165	20
$^{100}\text{Y}$	0,6	10	2,17	10	0,42	10	0,92	20
$^{101}\text{Y}$	0,25	10	0,863	10	0,125	15	0,272	30
$^{102}\text{Y}$	-	-	0,36	20	-	-	$5,0 \cdot 10^{-2}$	30
$^{103}\text{Y}$	-	-	0,115	30	-	-	$1 \cdot 10^{-2}$	50
$^{103}\text{Nb}$	2,1	3	5,7	5	3,0	3	3,84	10
$^{104}\text{Nb}$	0,724	6	3,85	10	1,5	3	2,41	20
$^{105}\text{Nb}$	0,26	6	2,3	20	0,53	6	1,0	20
$^{106}\text{Nb}$	0,14	10	0,9	20	0,14	10	0,315	30
$^{107}\text{Nb}$	-	-	0,25	20	$8 \cdot 10^{-3}$	10	$6 \cdot 10^{-2}$	30
$^{109}\text{Tc}$	-	-	0,12	20	0,55	-	0,9	-
$^{110}\text{Tc}$	-	-	$6 \cdot 10^{-2}$	30	-	-	0,21	-
$^{128}\text{In}$	$5 \cdot 10^{-2}$	5	0,211	23	0,1	10	0,13	10

Table 3. (cont.)

Nuclide	$^{235}\text{U}$		$^{238}\text{U}$		$^{239}\text{Pu}$		$^{241}\text{Pu}$	
	$q$	$\Delta q$	$q$	$\Delta q$	$q$	$\Delta q$	$q$	$\Delta q$
$^{129}\text{In}$	$5 \cdot 10^{-2}$	5	0,251	23	$7,6 \cdot 10^{-2}$	10	0,13	20
$^{130}\text{In}$	$3,5 \cdot 10^{-2}$	20	0,199	23	0,05	5	0,11	10
$^{131}\text{In}$	$2,4 \cdot 10^{-2}$	30	0,13	30	$6 \cdot 10^{-3}$	10	$5,8 \cdot 10^{-2}$	30
$^{132}\text{In}$	$4,1 \cdot 10^{-3}$	30	$5,7 \cdot 10^{-2}$	30	-	-	$2,8 \cdot 10^{-2}$	100
$^{134}\text{In}$	$4,1 \cdot 10^{-3}$	20	0,343	20	-	-	$8,1 \cdot 10^{-2}$	50
$^{134}\text{Sb}$	0,625	4	3,26	20	0,125	4	1,60	30
$^{135}\text{Sb}$	0,18	6	1,33	35	$6,8 \cdot 10^{-2}$	10	0,458	20
$^{136}\text{Sb}$	$6,15 \cdot 10^{-2}$	10	0,46	35	$2,6 \cdot 10^{-3}$	10	0,105	50
$^{137}\text{Sb}$	$4,7 \cdot 10^{-2}$	30	$9 \cdot 10^{-2}$	50	-	-	$1,33 \cdot 10^{-2}$	50
$^{136}\text{Te}$	1,91	5	4,81	5	0,545	10	3,11	20
$^{137}\text{Te}$	0,56	10	2,4	10	$9,0 \cdot 10^{-2}$	10	1,09	30
$^{138}\text{Te}$	0,14	10	0,932	20	$1,08 \cdot 10^{-2}$	20	0,277	30
$^{139}\text{Te}$	$3,3 \cdot 10^{-2}$	-	0,33	30	-	-	0,05	50
$^{137}\text{I}$	3,27	6	5,35	15	2,433	4	4,345	6
$^{138}\text{I}$	1,78	6	3,99	20	1,175	8	2,47	8
$^{139}\text{I}$	0,98	6	2,767	20	0,314	40	1,113	8
$^{140}\text{I}$	0,18	20	1,113	40	$5,9 \cdot 10^{-2}$	20	0,333	20
$^{141}\text{I}$	$4,1 \cdot 10^{-2}$	30	0,306	50	$5 \cdot 10^{-3}$	40	$5 \cdot 10^{-2}$	40
$^{141}\text{Xe}$	1,44	5	3,59	10	0,465	10	1,86	20
$^{142}\text{Xe}$	0,48	5	1,69	10	0,135	10	0,67	20
$^{143}\text{Xe}$	0,12	10	0,4	50	$2 \cdot 10^{-2}$	-	0,16	30
$^{144}\text{Xe}$	-	-	0,1	50	-	-	$2,5 \cdot 10^{-2}$	40
$^{141}\text{Cs}$	4,5	4	6,75	4	3,3	4	4,4	6
$^{142}\text{Cs}$	2,05	4	4,9	4	1,49	4	3,0	4
$^{143}\text{Cs}$	1,45	4	3,3	20	0,544	5	1,66	10
$^{144}\text{Cs}$	0,52	10	1,95	30	0,119	10	0,58	10
$^{145}\text{Cs}$	0,101	20	0,64	30	0,0205	10	0,149	20
$^{146}\text{Cs}$	$1,1 \cdot 10^{-2}$	30	0,14	50	-	-	$2,2 \cdot 10^{-2}$	20
$^{147}\text{Cs}$	-	-	$2 \cdot 10^{-2}$	50	-	-	$3 \cdot 10^{-3}$	50

spectrum at 14 Mev in the maximum-value region is close to the  $^{235}\text{U}$  fragment spectrum, while in the symmetrical fission region the yield increases by 1.5-2 orders.

Calculation of delayed neutron yield per fission. The delayed neutron yield per fission event,  $\nu_d$ , is calculated as the sum of the products of the probability of emission of a neutron per disintegration  $P_n$  and the cumulative emitter yield  $q$ :

$$\nu_d = \sum P_n q_i \quad (5)$$

For the majority of nuclei, the predominating role is played by relatively few emitter nuclides. Thus, according to our calculations, in the

Table 4. Delayed neutron yield (per 100 fission events).

Nuclide	Present study	Measurement [12,20] or evaluation [18]	Calculation	
			[3]	[2]
Thermal neutron fission				
$^{229}\text{Th}$	$1,75\pm0,25$	—	—	—
$^{233}\text{U}$	$0,756\pm0,08$	$0,74\pm0,04$ [12]	$0,87\pm0,1$	$0,85\pm0,07$
$^{235}\text{U}$	$1,678\pm0,09$	$1,67\pm0,07$ [12] $1,62\pm0,05$ [18]	$1,86\pm0,1$	$1,77\pm0,08$
$^{239}\text{Pu}$	$0,644\pm0,06$	$0,65\pm0,05$ [12] $0,628\pm0,036$ [18]	$0,70\pm0,06$	$0,77\pm0,04$
$^{241}\text{Pu}$	$1,485\pm0,16$	$1,57\pm0,15$ [12] $1,52\pm0,11$ [18]	$1,46\pm0,11$	$1,58\pm0,11$
$^{243}\text{Cm}$	$0,35\pm0,08$	—	—	—
$^{245}\text{Cm}$	$0,59\pm0,05$	$0,59\pm0,04$ [12]	—	—
$^{247}\text{Cm}$	$1,15\pm0,15$	—	—	—
Fast neutron fission				
$^{232}\text{Th}$	$5,15\pm0,31$	$5,27\pm0,40$ [12] $5,31\pm0,23$ [18]	$5,45\pm0,74$	$4,76\pm0,34$
$^{232}\text{U}$	$0,48\pm0,06$	$0,44\pm0,03$ [12]	—	—
$^{233}\text{U}$	$0,86\pm0,08$	$0,779\pm0,043$ [20] $0,731\pm0,036$ [18]	$0,93\pm0,12$	$0,92\pm0,09$
$^{235}\text{U}$	$1,712\pm0,154$	$1,67\pm0,07$ [12] $1,673\pm0,036$ [18]	$2,04\pm0,23$	$1,98\pm0,18$
$^{236}\text{U}$	$2,133\pm0,24$	$2,21\pm0,24$	$2,36\pm0,28$	$2,26\pm0,19$
$^{238}\text{U}$	$4,25\pm0,51$	$4,60\pm0,25$ [12] $4,39\pm0,10$ [18]	$3,52\pm0,3$	$3,51\pm0,27$
$^{237}\text{Np}$	$1,15\pm0,15$	$1,22\pm0,03$ [20]	$1,24\pm0,15$	$1,28\pm0,13$
$^{239}\text{Pu}$	$0,64\pm0,092$	$0,65\pm0,05$ [12] $0,63\pm0,016$	$0,65\pm0,08$	$0,72\pm0,09$
$^{240}\text{Pu}$	$0,905\pm0,154$	$0,911\pm0,041$ [20] $0,95\pm0,08$ [18]	$0,84\pm0,1$	$0,92\pm0,11$
$^{241}\text{Pu}$	$1,31\pm0,24$	$1,60\pm0,09$ [20]	$1,37\pm0,11$	$1,41\pm0,14$
$^{242}\text{Pu}$		$1,52\pm0,11$ [18]	—	—
$^{242}\text{Pu}$	$1,86\pm0,51$	$2,21\pm0,26$ [18]	$1,31\pm0,13$	$1,41\pm0,14$
$^{241}\text{Am}$	$0,394\pm0,15$	$0,394\pm0,024$ [20]	—	—
14 MeV neutron fission				
$^{232}\text{Th}$	$3,03\pm0,29$	$2,85\pm0,13$ [18]	$3,55\pm0,87$	$3,03\pm0,29$
$^{233}\text{U}$	$0,605\pm0,07$	$0,422\pm0,025$ [18]	$0,87\pm0,1$	$0,85\pm0,07$
$^{235}\text{U}$	$0,98\pm0,1$	$0,927\pm0,029$ [18]	$0,98\pm0,12$	$0,98\pm0,10$
$^{238}\text{U}$	$2,49\pm0,32$	$2,13\pm0,08$ [18]	$2,71\pm0,29$	$2,69\pm0,21$
$^{239}\text{Pu}$	$0,4\pm0,067$	$0,417\pm0,016$ [18]	$0,33\pm0,06$	$0,39\pm0,06$

case of  $^{235}\text{U}$  the combined contribution from 21 emitters represents 89%. In that of  $^{233}\text{U}$ , 92% of the contribution to  $\nu_d$  is furnished by 14 emitters.

On the basis of calculations using formula (5) the authors have derived (Table 4) values for the yield  $\nu_d$  in the case of thermal neutron fission of  $^{233}, ^{235}\text{U}$ ,  $^{239}, ^{241}\text{Pu}$ ,  $^{229}\text{Th}$ , and  $^{243}, ^{245}, ^{247}\text{Cm}$ , of the fission

spectrum neutron fission of  $^{232}\text{Th}$ ,  $^{232,233,235,236,238}\text{U}$ ,  $^{237}\text{Np}$ ,  $^{239,240,241,242}\text{Pu}$  and  $^{241}\text{Am}$ , and of 14 MeV neutron fission of  $^{232}\text{Th}$ ,  $^{233,235,238}\text{U}$ , and  $^{239}\text{Pu}$ . In addition, Table 4 shows the results of microscopic measurements and evaluations, and also - by way of comparison - the calculated yields  $\nu_d$  taken from Refs. [2, 3].

The experimental works have been selected largely on a subjective basis. Here, the principal aim was to show the scale of measurement error. In Ref. [18] evaluation of  $\nu_d$  is in essence not performed, averaging being carried out of the experimental results published up to 1978. Thus, for  $^{235}\text{U}$  the  $\nu_d$  value of 1.62 is based on a single study [19]. In our opinion this value is too low, which is indeed confirmed by a later experiment [12].

In Ref. [2] the  $\nu_d$  value for  $^{235}\text{U}$  is 5% higher than in the present study. It is possible that this is connected with exaggeration of the contribution of yttrium (3.9% with us, about 7.6% in Ref. [2]), and also of barium and lanthanum. Experimental data [9] show that the contribution of yttrium is still lower (about 2.8%), while that of barium and lanthanum can be ignored.

Let us look in greater detail at the effects of the strontium and yttrium contribution on the discrepancy in the value of  $\nu_d$ . According to study [9],  $^{97}\text{Sr}$  is not a delayed neutron emitter, the contribution of  $^{99}\text{Sr}$  should be reduced by a factor of 10, and that of  $^{98}\text{Sr}$  by a factor of 1.7. All this reduces the value of the yield for  $^{235}\text{U}$  by 0.75%. In the case of  $^{97}\text{Y}$  the results of Ref. [9] agree with our values for the ground state of this nucleus.

As regards the isomeric state, the size of the fission yield is not clear. For  $^{98}\text{Y}$  our results should be less by a factor of three, and for  $^{99}\text{Y}$  by 20%, which results in a reduction in yield  $\nu_d$  for  $^{235}\text{U}$  by a further 1%. Overall, in the light of experiments [11] the yield value should be reduced to 1.65. However, it is possible that in the present study the

probability  $P_n$  for certain emitters is a few percent lower, and therefore our figure for the yield may be regarded as reasonable. Study [2] adopts larger  $P_n$  values for  $^{97,98}\text{Y}$  than in our work; substitution of experimentally evaluated probabilities  $P_n$  reduces the yield to about 1.67 in accordance with our data.

The  $\nu_d$  value for  $^{239}\text{Pu}$  in study [2] is greater than ours by 12%, while the contribution of yttrium amounts to 6.6% in our work and 12.5% in study [2].

As will be seen from Table 4, the agreement of the  $\nu_d$  value with the experiment performed in the study in question proves to be good. Of note is the excessively high figure for  $^{235}\text{U}$  obtained in Ref. [3]. The value for  $^{241}\text{Pu}$  both in the present work and in Ref. [3] comes out as too low. Regarding the results in Ref. [2], the value for  $^{241}\text{Pu}$  close to the experimental figure emerges as a result of the excessive contribution of yttrium and possibly, of niobium and technetium. In the case of fission neutrons the fragment spectrum has been a good deal more poorly studied. It is probable that precisely this leads to the discrepancy between all theoretical evaluations and experimental results in respect of  $^{233}\text{U}$  and  $^{241}\text{Pu}$  fission. A surprising feature is the good agreement with experimental values of all calculations for 14 MeV (there is a certain discrepancy only in the case of  $^{233}\text{U}$ ).

It is to be noted that the part played by uninvestigated emitters is not very great. Below we give the contribution  $(\Delta\nu_d)_u - \nu_d$  (in percent), governed in our calculations by evaluation of uninvestigated emitters: for  $^{233}\text{U}_{th} - 2.4$ ;  $^{235}\text{U}_{th} - 4.4$ ;  $^{239}\text{Pu}_{th} - 9$ ;  $^{241}\text{Pu}_{th} - 10$ ;  $^{238}\text{U}_f - 10$ ;  $^{232}\text{Th}_f - 4$ , where the index "u" relates to uninvestigated emitters; th represents thermal neutron fission; and f represents fissioning spectrum neutron fission. As can be seen, this contribution increases in the case of heavier fissionable nuclides, associated with the shift of the fragment mass spectrum into the uninvestigated strontium-technetium region.



The error  $\Delta v_d$ , given in Table 4, was calculated using the standard procedure:

$$\frac{\Delta v_d}{v_d} = \left\langle \sum_i \left\{ \left[ \left( \frac{\Delta P_i}{P_i} \right)^2 + \left( \frac{\Delta q_i}{q_i} \right)^2 \right] \left( \frac{v_i}{v} \right)^2 \right\} \right\rangle^{1/2},$$

where  $v_i = P_i q_i$  is the contribution of the  $i$ -th emitter to the yield  $v_d$ .

The calculation was carried out for only 12 host emitters. Their contribution (in per cent) to the yield  $v_d$  for various fissionable nuclides is given below: for  $^{233}\text{U}_{th}$  - 87,  $^{235}\text{U}_{th}$  - 76,  $^{239}\text{Pu}_{th}$  - 80,  $^{241}\text{Pu}_{th}$  - 63,  $^{238}\text{U}$  - 80,  $^{245}\text{Cm}_{th}$  - 75,  $^{235}\text{U}_f$  - 78,  $^{236}\text{U}_f$  - 75,  $^{238}\text{U}_f$  - 60,  $^{232}\text{Th}_f$  - 69,  $^{237}\text{Np}_f$  - 77,  $^{239}\text{Pu}_f$  - 76.

As will be seen, the contribution due to the host emitters represents 75-80%, and drops to 60% only in the case of  $^{238}\text{U}$  and  $^{241}\text{Pu}$ . For the 12 fragments considered, the error  $\Delta P_n / P_n$  represents less than 10%, with the possible exception of  $^{85}\text{As}$ . In the majority of cases, except for  $^{235}\text{U}_{th}$  and  $^{239}\text{Pu}$  fission, this error is much less than  $\Delta q_i / q_i$ . The latter quantity also gives the basic contribution to  $\Delta v_d / v_d$ . The overall error is much less than the individual  $\Delta \gamma_i / \gamma_i$  values, and hence in respect of emitters with a low  $\gamma_i / v_d$  weight and known  $P_n$  it is taken that the overall error is 10%, while for uninvestigated emitters it is 100%.

The total error is calculated according to the formula

$$\frac{\Delta v_d}{v_d} = \left[ \frac{(\Delta v)_{12}^2}{v_d^2} + \frac{(\Delta v)_i^2}{v_d^2} + \frac{(\Delta v)_u^2}{v_d^2} \right]^{1/2},$$

where the index "i" relates to investigated emitters.

By way of example let us give the calculation for the error in the yield  $v_d$  for  $^{235}\text{U}_{th}$ . In this case 76% of the contribution to  $v_d$  is furnished by 12 emitters, while the remaining 24% are distributed as follows: 19.6% - investigated fragments and 4.4% - uninvestigated fragments. The 12 host emitters are responsible for a small error, since the values for  $\Delta q_i / q_i$  are small, namely  $(\Delta v)_{12} / v_d \sim 0.020$ . It will further be seen that  $(\Delta v)_i / v_d = 0.0196$ , and  $(\Delta v)_u / v_d = 0.044$ . Thus,  $\Delta v_d = 0.052 v_d$ .

The values obtained in the present study for the total delayed fission neutron yield are in good agreement with the results of macroscopic measurements. Of the 25 cases considered, in 23 of them the difference does not exceed the limits of calculational imprecision and in no case is the combined measurement and calculational error exceeded. There is no systematic deviation. This points to the reliability of the evaluation-based values for the probability of neutron emission by fission fragment nuclei and for the yield of these fragments. The results obtained may also be used for calculating other integral properties of delayed neutrons. At the same time the accuracy of the experimental data on the emitter fragments does not permit the derivation of yield  $\nu_d$  with an accuracy better than direct measurements. The imprecision of calculation, as a rule, exceeds the macroscopic measurement error by a factor of 1.5-2.

#### REFERENCES

1. England T.R., Schenter R.E., Schmittroth W.B. Delayed neutron calculation using ENDF/B-V data//Proc. ANS/APS Int. conf. nucl. cross-sections for technology: NBS Special Publication. Knoxville, 1979. P.594.
2. England T.R., Wilson W.B., Schenter R.E. Aggregate delayed neutron intensities and spectra using augmented ENDF/B-V precursor data//Nucl. Sci. and Engng. 1983. V.85. P.139.
3. Reeder P.L., Warner R.A. Distribution of delayed neutron yields versus proton, neutron and mass numbers//Ibid. 1984. V.87. P.181.
4. Manevich L.G., Nemirovskij P.Eh., Yudkevich M.S., Delayed neutron constants: Preprint IAEh-4308/4, Moscow, 1986.
5. Rudstam G. Status of delayed neutron data// Fission product nuclear data. Vienna: IAEA, 1977. V.II. P.567.
6. Rudstam G. Report for the meeting on delayed neutrons. Vienna: IAEA, 1979.
7. Aknelt K., Hoff P., Lund E.e.a. Delayed neutron emission probabilities of the precursors  $^{89,90,91}\text{Br}$  and  $^{139,140,141}\text{J}$ //Z.Phys. 1979. Bd A290. S.331.
8. Ristori C., Wunsh K.D., Decker R. Half-lives and delayed neutron emission probabilities of short-lived Rb and Cs precursors//Ibid. S.311.
9. Reeder P.L., Warner R.A. Delayed neutron precursors at masses 97-99 and 146-148//Phys.Rev. 1983. V.C28. P.1740.
10. Rudstam G. Six-group representation of the energy spectra of delayed neutron from fission// Nucl.Sci.and Engng. 1982. V.80. P.238.
11. England T.R., Mann F.H., Schreiber M., Schenter R.E. Compilation on neutron data: Antwerp. Conf. 1982.
12. Waldo R.W., Karam R.A., Meyer R.A. Delayed neutron yields time dependent measurements and predictive model//Phys.Rev. 1981. V.C23. P.1113.
13. Crancon J., Ristori C., Ohm H. e.a. Half-lives and  $P_n$  values of delayed-neutron precursors in the mass chains 85-87, 92, 135, 136 and 145//Z.Phys. 1978. Bd A287. S.45.
14. Wapstra A.H., Bos K. The 1977 Atomic mass evaluation//Atomic Data and Nuclear Data Tables. 1977. V.19. P.173.
15. Kratz K.L., Herman L.//Z.Phys. 1973. Bd A263. S.435.

16. Blachot J. Status of decay data of fission product. Fission product nuclear data (FPND)-1977. Vienna: IAEA, 1978. V.II. P.487.
17. Rider B.F., Meek M.E. Compilation of fission product yields. 1977: NEDO-12154-2(USA).
18. Tuttle R.J. Delayed-neutron in nuclear fission: Proc.of the consultants meeting on delayed neutron properties. Vienna: IAEA, 1979: INDC(NDS)-107.
19. Keepin D.R., Physical principles and kinetics of nuclear reactors. Moscow, Atomizdat, 1967.
20. Benedetti G., Cesari A., Sangiust V.//Sci.and Engng. 1982. V.80. P.379.

Paper received by editors on 30 January 1987.



## CALCULATION OF INTEGRAL DELAYED NEUTRON PROPERTIES

### Part 2. Group constants and reactivity

L.G. Manevich, P.Eh. Nemirovskij, M.S. Yudkevich

CALCULATION OF INTEGRAL DELAYED NEUTRON PROPERTIES. PART 2. DELAYED NEUTRON PARAMETERS AND REACTIVITY. Using the fission-product delayed neutron precursor data, six delayed neutron groups for six fissionable nuclides were obtained. Comparison with known sets of delayed neutron parameters was performed in terms of reactor kinetics calculations.

Recently there has been a substantial increase in the volume of information available on fission product yields and on their decay properties. This makes it possible to perform fairly accurate calculations of the quantities described by the overall properties of the individual nuclei. In a previous work [1] we calculated the total delayed neutron yield  $\nu_d$  for a number of fissionable nuclei, adopting such a microscopic approach. Satisfactory agreement of the values obtained with the results of macroscopic measurements gives grounds for asserting the reliability of the data used in Ref. [1] and the assumptions made. In the present study, these same data are used for calculating the time dependence of neutron yield after irradiation of fissionable nuclei. Effective six-group constants were derived. Their comparison with the data obtained by other authors was carried out in connection with the measurement of reactor reactivity by the method of inverse solution of kinetics equations. Mean group energies for delayed neutrons were calculated, corresponding to the six-group constants obtained.

#### Calculation of neutron activity function and analysis of its accuracy.

We shall describe the neutron activity function  $f(t)$  as the time dependence of delayed neutron yield from a mixture of fragments formed as a result of instantaneous irradiation of a fissionable nucleus. In order to derive this function it is necessary to know the yields of neutron emitting nuclei and their half-lives. The yields were evaluated in Ref. [1], and the lifetime data were taken from the handbook [2], as supplemented by Ref. [3]. The half-lives of long-lived emitters ( $^{87}\text{Br}$ ,  $^{137}\text{I}$ ) are known with an accuracy

better than about 1%. For a number of short-lived emitters ( $^{88}\text{As}$ ,  $^{101}\text{Y}$ ) the half-life is completely unknown, but their contribution is small, and hence any scheme in the nature of  $0.1 < T_{1/2} < 1$  s will have no significant effect on the function  $f(t)$ .

The function in question is derived by summation of the decay curves of the individual emitters. The decay of an individual emitter is described by an exponential curve only in cases where all its precursors arising immediately upon fission have a much shorter half-life. Otherwise, the law of radioactive disintegration represents the sum of the exponential term with a coefficient corresponding to the direct yield of the given nuclide upon fission and of the terms arising from its precursors.

The precursors of a nucleus with  $Z, A$  may be nuclei with  $Z-1, A$  and  $Z-2, A$ , being transformed into nuclei with  $Z, A$  as a result of  $\beta$ -decay, and a nucleus with  $Z-1, A+1$ , emitting a delayed neutron after  $\beta$ -decay. However, the last two mentioned nuclei represent a small contribution and they can, without serious error, always be combined with nuclei having  $Z-1, A$  or  $Z, A$ . Then the neutron activity curve for the individual emitter having precursors is described by the formula

$$f_A^Z(t) = P_A^Z \left\{ \lambda_A^Z q_A^Z \exp(-\lambda_A^Z t) + q_A^{Z-1} (1 - P_A^{Z-1}) \frac{\lambda_A^Z \lambda_A^{Z-1}}{\lambda_A^{Z-1} - \lambda_A^Z} [\exp(-\lambda_A^Z t) - \exp(-\lambda_A^{Z-1} t)] \right\}, \quad (1)$$

where  $\lambda$  is the decay constant.

Table 1 quotes the ratio of individual yield for those nuclei for which the precursor plays a part.

It is known that for longer times,  $t \gg T_{1/2}$  ( $^{137}\text{I}$ ), the activity decay curve behaves as an exponential curve with the decay constant of  $^{87}\text{Br}$  ( $\lambda = 0.01245 \text{ s}^{-1}$ ). However, for  $^{87}\text{Br}$  there is an additional factor  $\beta[\lambda_{\text{Br}}/(\lambda_{\text{I}} - \lambda_{\text{Br}}) + 1]$ , which in the case of thermal neutron fission of  $^{235}\text{U}$ , for example, represents 4%. This must be taken into account when constituting the group constants.

**Table 1.** Ratio between individual and cumulative yields upon fission of various nuclei.

Nuclide	<sup>232</sup> Th	<sup>233</sup> U	<sup>235</sup> U	<sup>238</sup> U	<sup>239</sup> Pu	<sup>241</sup> Pu
<sup>85</sup> As	0,894	1,0	1,0	0,9	1,0	0,98
<sup>87</sup> Br	0,34	0,73	0,613	0,277	0,792	0,57
<sup>88</sup> Br	0,515	0,88	0,78	0,52	0,905	0,79
<sup>89</sup> Br	0,77	0,93	0,93	0,73	0,982	0,92
<sup>93</sup> Rb	0,57	0,91	0,85	0,55	0,96	0,78
<sup>94</sup> Rb	0,75	1	0,92	0,775	0,98	0,913
<sup>98</sup> Y	0,6	0,91	0,72	0,63	0,9	0,79
<sup>99</sup> Y	0,8	0,99	0,86	0,82	0,97	0,92
<sup>137</sup> I	0,675	0,95	0,829	0,55	0,963	0,745
<sup>138</sup> I	0,83	0,985	0,921	0,77	0,99	0,89
<sup>139</sup> I	0,92	1,0	0,967	0,88	1,0	0,95
<sup>143</sup> Cs	0,88	1,0	0,92	0,93	0,96	0,9

Let us consider the error of the function  $f(t)$ . Neglecting the difference in the individual contributions from a simple exponential curve (except <sup>238</sup>U and <sup>232</sup>Th it does not exceed 5%), the error of each term in expression (1)

$$\Delta f_i(t) = (\lambda_i \Delta \gamma_i + \gamma_i \Delta \lambda_i - \lambda_i \gamma_i t \Delta \lambda_i) \exp(-\lambda_i t).$$

As a rule, the error in  $\gamma_i$  (where  $\gamma = pq$ ) is greater than in  $\lambda_i$ . However, when  $\lambda_i t \gg 1$ , the term with  $\Delta \lambda_i$  can assume decisive importance. Since the errors in the parameters  $\lambda_i$  and  $\gamma_i$  are independent,

$$D(f_i) = [(\Delta \gamma_i / \gamma_i)^2 + (\Delta \lambda_i / \lambda_i)^2 (1 - \lambda_i t)^2]$$

and

$$\Delta f(t) = \left\{ \sum_i \frac{[f_i(t)]^2}{[f(t)]^2} D(f_i) \right\}^{1/2} \quad (2)$$

Calculation of the function  $f(t)$  was performed for the nuclides <sup>233</sup>U, <sup>235</sup>U, <sup>238</sup>U and <sup>239</sup>Pu, <sup>241</sup>Pu. The result for <sup>235</sup>U upon thermal neutron fission is given in Table 2. Description of the function using formula (1) is cumbersome. It is preferable to resort to groups with effective decay constants  $\lambda$  and yield  $a$ . Twenty groups were selected and it was then shown that the accuracy of approximation of the function  $f(t)$  is not poorer than 1%. For <sup>235</sup>U this can be seen from Table 2.

**Table 2.** Calculational function  $f(t)$  and error of 20-group approximation for  $^{235}\text{U}$ .

Time $t, \text{ s}$	$f(t) \cdot 10^5$	Error $\eta, \%$	Time $t, \text{ s}$	$f(t) \cdot 10^5$	Error $\eta, \%$
0	792 $\pm$ 40	0,8	25	7,5 $\pm$ 0,3	-0,2
1	282 $\pm$ 12	-1,3	30	5,8 $\pm$ 0,3	-0,4
2	172 $\pm$ 6,2	-0,68	35	4,6 $\pm$ 0,2	-0,5
3	123,8 $\pm$ 4,2	-0,66	40	3,8 $\pm$ 0,2	-0,65
4	94,2 $\pm$ 3,1	-0,45	50	2,7 $\pm$ 0,14	-0,9
5	74,3 $\pm$ 2,3	-0,36	60	1,97 $\pm$ 0,10	-1
6	59,8 $\pm$ 1,8	-0,3	75	1,27 $\pm$ 0,06	-1,21
8	40,8 $\pm$ 1,3	-0,16	100	0,65 $\pm$ 0,03	-1,26
10	29,6 $\pm$ 0,9	-0,06	125	0,35 $\pm$ 0,02	-1,16
12	22,5 $\pm$ 0,6	-0,05	150	0,20 $\pm$ 0,01	-0,99
16	14,5 $\pm$ 0,5	0,07	175	0,12 $\pm$ 0,01	-0,73
20	10,4 $\pm$ 0,4	-0,1	200	0,078 $\pm$ 0,004	-0,5

The twenty-group constants for the above nuclei are given in Table 3.

We will now describe how the groups were chosen:

- The first group consists of pure  $^{87}\text{Br}$ ;
- The second group comprises  $^{137}\text{I}$  and  $^{141}\text{Cs}$  (of similar half-life), whose contribution to this group represents about 0.7% (here and henceforth we indicate the contributions to the group for thermal neutron fission of  $^{235}\text{U}$ );
- The third group comprises, in addition to the host emitter  $^{88}\text{Br}$ , also  $^{136}\text{Te}$ , whose contribution represents about 11%. According to Ref. [2] the constant  $\lambda(^{136}\text{Te})$  differs from  $\lambda(^{88}\text{Br})$  by 20%, but according to Ref. [4] the constant  $\lambda(^{136}\text{Te})$  is 10% more and consequently the difference is less. Furthermore, this group includes the problematic  $^{103}\text{Nb}$ , whose half-life is taken from Ref. [5].

Its contribution is 1.8%, and therefore if it has a somewhat different half-life, this will not cause any substantial error since it falls within the limits of the error for  $^{88}\text{Br}$ :

- The fourth group comprises  $^{138}\text{I}$  and  $^{134}\text{S}$ . The half-life of  $^{134}\text{S}$  is 50% greater than that of  $^{138}\text{I}$ , but its contribution is 140 times less, i.e. it can be assumed without serious error that



Table 3. 20-group constants  $\lambda$  and  $a$  for various fissionable nuclei.

No. of group	$\lambda, \text{c}^{-1}$	$a \cdot 10^4$ on thermal neutron fission				$a \cdot 10^4$ on fast neutron fission		
		$^{233}\text{U}$	$^{235}\text{U}$	$^{239}\text{Pu}$	$^{241}\text{Pu}$	$^{235}\text{U}$	$^{238}\text{U}$	$^{239}\text{Pu}$
1	0,01245	6,1 $\pm$ 0,4	5,35 $\pm$ 0,30	1,8 $\pm$ 0,1	1,64 $\pm$ 0,11	5,6 $\pm$ 0,4	4,12 $\pm$ 0,25	2,0 $\pm$ 0,2
2	0,0282	10,3 $\pm$ 0,8	21,6 $\pm$ 1,4	15,8 $\pm$ 0,8	28,9 $\pm$ 2,2	22,2 $\pm$ 2	36,4 $\pm$ 3,5	12,3 $\pm$ 0,9
3	0,040	0,4 $\pm$ 0,1	1,7 $\pm$ 0,3	0,5 $\pm$ 0,1	2,7 $\pm$ 0,3	1,7 $\pm$ 0,3	4,3 $\pm$ 0,5	0,5 $\pm$ 0,2
4	0,0431	11,1 $\pm$ 0,8	13,6 $\pm$ 0,8	4,0 $\pm$ 0,2	4,6 $\pm$ 0,4	15,1 $\pm$ 1,4	14,2 $\pm$ 1,2	4,7 $\pm$ 0,4
5	0,107	2,9 $\pm$ 0,3	9,3 $\pm$ 0,8	6,0 $\pm$ 0,4	13,0 $\pm$ 1,3	9,0 $\pm$ 0,9	22 $\pm$ 2	5,5 $\pm$ 0,5
6	0,1185	3,2 $\pm$ 0,2	5,8 $\pm$ 0,3	2,6 $\pm$ 0,2	2,9 $\pm$ 0,5	5,5 $\pm$ 0,5	7,2 $\pm$ 0,7	2,4 $\pm$ 0,2
7	0,158	11,5 $\pm$ 0,8	19,5 $\pm$ 0,8	5,1 $\pm$ 0,4	6,0 $\pm$ 0,8	25,2 $\pm$ 2,0	29,7 $\pm$ 4,0	5,2 $\pm$ 0,5
8	0,251	10,0 $\pm$ 0,8	20,1 $\pm$ 1	8,6 $\pm$ 0,5	15 $\pm$ 3	19,4 $\pm$ 2	39,0 $\pm$ 4,5	8,6 $\pm$ 0,9
9	0,287	2,1 $\pm$ 0,2	9,5 $\pm$ 0,8	3,0 $\pm$ 0,2	10,8 $\pm$ 1	9,2 $\pm$ 0,9	27,5 $\pm$ 3,0	1,8 $\pm$ 0,3
10	0,344	3,2 $\pm$ 0,4	5,6 $\pm$ 1	2,1 $\pm$ 0,4	3,7 $\pm$ 0,5	5,6 $\pm$ 1	11,1 $\pm$ 1,5	3,0 $\pm$ 0,4
11	0,372	7,1 $\pm$ 0,7	17,4 $\pm$ 1,3	4,3 $\pm$ 0,5	10,0 $\pm$ 0,9	16,5 $\pm$ 2	44,2 $\pm$ 5,0	5,3 $\pm$ 0,4
12	0,405	0,6 $\pm$ 0,2	3,1 $\pm$ 0,4	1,0 $\pm$ 0,2	8,2 $\pm$ 0,8	3,0 $\pm$ 0,4	20,7 $\pm$ 2,5	0,7 $\pm$ 0,1
13	0,495	1,2 $\pm$ 0,2	5,0 $\pm$ 1,5	1,7 $\pm$ 0,2	4,9 $\pm$ 1	4,3 $\pm$ 0,5	13,3 $\pm$ 2,5	2,1 $\pm$ 0,2
14	0,665	0,6 $\pm$ 0,2	2,8 $\pm$ 0,5	1,2 $\pm$ 0,2	4,5 $\pm$ 0,8	2,6 $\pm$ 0,4	13,5 $\pm$ 3,0	1,6 $\pm$ 0,2
15	0,845	0,3 $\pm$ 0,1	3,0 $\pm$ 0,6	1,1 $\pm$ 0,2	7,4 $\pm$ 0,9	3,6 $\pm$ 0,5	17,4 $\pm$ 3,0	1,5 $\pm$ 0,2
16	1,15	0,35 $\pm$ 0,05	4,5 $\pm$ 0,5	1,0 $\pm$ 0,2	7,5 $\pm$ 1	4,1 $\pm$ 0,8	20,6 $\pm$ 3,0	1,2 $\pm$ 0,2
17	1,29	1,4 $\pm$ 0,2	4,2 $\pm$ 0,4	0,5 $\pm$ 0,2	2,0 $\pm$ 0,5	3,4 $\pm$ 0,6	16,9 $\pm$ 3,0	0,6 $\pm$ 0,1
18	1,8	2,0 $\pm$ 0,2	7,5 $\pm$ 0,4	2,6 $\pm$ 0,2	7,6 $\pm$ 1	7,5 $\pm$ 1	35,5 $\pm$ 5,0	3,1 $\pm$ 0,3
19	2,3	1,1 $\pm$ 0,2	4,0 $\pm$ 1,5	1,1 $\pm$ 0,2	4,0 $\pm$ 0,5	4,6 $\pm$ 1	23 $\pm$ 5	1,1 $\pm$ 0,2
20	3,6	0,2 $\pm$ 0,1	4,4 $\pm$ 1	0,45 $\pm$ 0,10	3,2 $\pm$ 0,5	3,1 $\pm$ 0,5	23 $\pm$ 6	0,7 $\pm$ 0,2

the constant  $\lambda$  of this group is equal to the  $\lambda$  value for  $^{138}\text{I}$ ;

The fifth group comprises  $^{93}\text{Rb}$  and the two weak emitters  $^{87}\text{Se}$  and  $^{84}\text{As}$ . The contribution of the last two is practically compensated by the component from  $^{87}\text{Br}$  with a  $\lambda$  value corresponding to  $^{87}\text{Se}$ ;

The sixth group comprises  $^{89}\text{Br}$  and the nuclides of similar half-life  $^{97}\text{Y}$  and  $^{92}\text{Rb}$ . The last two make an approximately 2% contribution to the group.

Thus, all the groups considered above, with the exception of the third, are virtually pure single-component emitters. However, as from the seventh group the picture changes:

- The seventh group involves  $^{94}\text{Rb}$  and  $^{137}\text{Te}$ , the latter making an approximately 6% contribution, and also the negative term from formula (1) for  $^{137}\text{I}$ ;
- The eighth group (pure) comprises  $^{139}\text{I}$ ;
- The ninth group includes  $^{85}\text{As}$  and  $^{98}\text{Y}$ . The first has been measured with poor accuracy, and the second was calculated on the basis of certain assumptions. It has now been shown [6, 7] that  $^{98}\text{Y}$  has a substantially (4 times) shorter half-life and a lower probability value  $P$  than had previously been thought. However, the  $P$  value for  $^{85}\text{As}$  is so unreliable that the total difference can be attributed to this nuclide;
- The tenth group comprises the strong emitter  $^{90}\text{Br}$ , and  $^{92}\text{Kr}$  and  $^{143}\text{Cs}$  with very similar half-lives, and presumably also  $^{105}\text{Nb}$ . The last three emitters account for approximately 17% of the intensity of the group;
- The eleventh group comprises  $^{135}\text{Sn}$  and  $^{141}\text{Xe}$ ,  $^{142}\text{Cs}$ .

The composition of the remaining, extremely mixed, groups will not be given here. We shall observe only that if it is possible to identify the strongest emitter, the constant  $\lambda$  of the group is regarded as equal to its  $\lambda$  value. It is not possible to do this in the 15th, 17th, 19th and 20th groups. Furthermore, the 20th group includes two nuclides ( $^{88}\text{As}$ ,  $^{101}\text{Y}$ ) with indeterminate half-life. Their contribution accounts for 9% of the total intensity of the group, and the  $\lambda$  value is taken as  $3.5 \text{ s}^{-1}$ .

The six-group constant system for various nuclides. In reactor work it is now general practice to divide delayed neutron sources into six groups, each of which consists of components with similar half-lives. There are available numerous experimental and theoretical studies determining the disintegration constants  $\lambda_j$  and the contributions  $a_j$  of each group for various fissionable nuclei. The method of solving the problem consists of expansion of the measured or calculated function  $f(t)$  into six exponential

components. Widest use is made of the data from Ref. [8]. The set of constants obtained upon thermal neutron fission is recommended in the BNAB system of constants [9], and in the case of fast neutron fission in the ENDF/B files [10]. For both libraries it is recommended that the appropriate sets of constants be used throughout the energy range. Reference [3] is one of the latest experimental studies in which the measurements were conducted on the basis of a thermal neutron spectrum. Studies [4, 11] are of interest for purposes of comparison with our results, since in the studies in question the information was extracted from data on delayed neutron emitters.

An analysis was carried out on how known six-group constant systems permit the approximation of the neutron activity function derived in this work, in respect of various fissionable nuclei. In the case of  $^{235}\text{U}$ , only the data from Ref. [8] (thermal neutron fission) do not go beyond the limits of indeterminacy of the function. An extreme divergence of  $f(t)$  from the curve obtained in Study [5] is seen. These calculations likewise exaggerate the value of the total delayed neutron yield  $\nu_d$ . For  $^{239}\text{Pu}$  our data are in good agreement only with those of study [3]. The results of the other authors go far beyond the limits of error. For  $^{238}\text{U}$  the function  $f(t)$  is well described by the data of Ref. [8]. Study [3] predicts the same shape of curve as in study [8], but differs in respect of normalization (by about 10%) and is situated on the boundary of error. As before, the calculations [4, 11] give a poor description of the curve. The comparison carried out showed that for describing the values of  $f(t)$  obtained in the present work it is necessary to assemble one's sets of six-group constants.

It is clear that the task of approximating the function  $f(t)$  by the sum of the exponentials involves a multiple-value solution. However, the numerical analysis effected showed that with practically any physically reasonable set of constants  $\lambda_j$  it is possible to select a set  $a_j$  yielding a sufficiently accurate description of this function. In reactor dynamics calculations use is generally made of values for  $\lambda_j$  taken from

Table 4. 6-group constants.

Nuclide	Constant	No. of group					
		1	2	3	4	5	6
$^{233}\text{U}_{\text{th}}$	$\lambda_j$	0,01255	0,0345	0,139	0,317	1,30	2,90
	$a_j$	$0,065 \pm 0,001$	$0,209 \pm 0,006$	$0,192 \pm 0,014$	$0,228 \pm 0,015$	$0,050 \pm 0,009$	$0,013 \pm 0,004$
$^{235}\text{U}_{\text{th}}$	$\lambda_j$	0,01245	0,0305	0,111	0,301	1,14	3,01
	$a_j$	$0,053 \pm 0,001$	$0,322 \pm 0,008$	$0,337 \pm 0,019$	$0,632 \pm 0,026$	$0,225 \pm 0,019$	$0,105 \pm 0,009$
$^{235}\text{U}_f$	$\lambda_j$	0,01245	0,0317	0,115	0,311	1,40	3,87
	$a_j$	$0,057 \pm 0,001$	$0,355 \pm 0,010$	$0,363 \pm 0,027$	$0,660 \pm 0,044$	$0,230 \pm 0,037$	$0,045 \pm 0,019$
$^{238}\text{U}$	$\lambda_j$	0,01272	0,0301	0,104	0,310	1,13	3,40
	$a_j$	$0,046 \pm 0,001$	$0,483 \pm 0,022$	$0,522 \pm 0,067$	$1,629 \pm 0,134$	$1,086 \pm 0,142$	$0,481 \pm 0,089$
$^{239}\text{Pu}_{\text{th}}$	$\lambda_j$	0,01255	0,0301	0,124	0,325	1,12	2,69
	$a_j$	$0,019 \pm 0,001$	$0,197 \pm 0,005$	$0,154 \pm 0,012$	$0,198 \pm 0,020$	$0,051 \pm 0,017$	$0,024 \pm 0,008$
$^{241}\text{Pu}_{\text{th}}$	$\lambda_j$	0,0126	0,0294	0,117	0,352	1,60	3,60
	$a_j$	$0,018 \pm 0,001$	$0,348 \pm 0,006$	$0,249 \pm 0,014$	$0,574 \pm 0,019$	$0,274 \pm 0,017$	$0,024 \pm 0,009$

**Note:** The index th signifies fission by thermal neutrons, and f signifies fission by fissioning spectrum neutrons.

Ref. [8]. These sets are adopted likewise in this work, with the exception of the quantity  $\lambda_1$  for certain nuclei. The  $a_j$  sets of constants were derived according to the standard procedure of the least squares method [12]. In a computer program  $f(t)$  and  $\Delta f(t)$  were calculated with reference to formulae (1) and (2) over the range  $0 \leq t \leq 1000$  s.

The systems of constants obtained for various fissionable nuclei are presented in Table 4. They satisfactorily describe the function  $f(t)$ . Divergences of the approximating function do not go beyond the limits of  $\Delta f(t)$ . The six-group constants given in the table differ from those recommended by other authors, for example those of Refs. [3, 8], but do not contradict them; the difference is the same as the differences between the results of the various studies.

It should be stressed that the group constants obtained in the present work are the result of treatment of experimental data. The method of obtaining them differs from the traditional procedure only in the way of measuring the neutron activity curve of the function  $f(t)$ . In traditional methods recourse is had to the macroscopic approach, and in our work to the microscopic one.

Mean energies of delayed neutron groups. The satisfactory agreement of the results of calculating yield  $\nu_d$  [1] with experimental data makes it possible to apply the method of summing the contributions of the individual precursors to the problem of determining the energy distribution of delayed neutrons. References [4, 11] present the energy spectra of neutrons emitted by fission products. Here there are experimental data for 31 nuclei, while for the remaining nuclei use was made of theoretical evaluations. We used this information for calculating the mean energy of the delayed neutron groups.

Let us correlate each neutron-emitter nucleus with a specific group of the six-group concept, and let us set the boundaries between the groups at values of  $\lambda$  equal to the geometric mean between the  $\lambda_i$  of the preceding and following groups. Then the mean neutron energy is determined by the evident correlation  $E_j = 1/a_j \sum_i a_i \bar{E}_i$ , where the index  $i$  denotes the emitter belonging to the group. In performing the calculations the parameter  $a_i$  was taken from Ref. [1], and  $\bar{E}_i$  from Ref. [11]. The results of the present calculations in comparison with the data from Ref. [4] are given in Table 5.

When comparing the calculated group spectra obtained by various authors, it should be remembered that there is a certain indefiniteness in the breakdown of delayed neutrons by groups, since particular emitters may have a value of  $\lambda$  corresponding to the boundary value of the group time interval, and may be referable to one or other of the adjoining groups.

The calculations carried out by the authors for the majority of fissionable nuclides are in good agreement with the results of Refs. [4, 11] as regards the first four groups. The higher level of our mean energies in groups 5 and 6 in comparison with the corresponding values from Ref. [4] is quite natural, since precisely in these groups there is a contribution by poorly investigated nuclides, not included in the calculations in Ref. [4]. It should be noted that our calculations do not contradict the group breakdown of emitters performed in Ref. [4]; this is apparent from the close proximity of the corresponding mean group energies.

**Table 5.** Mean group energies for delayed neutrons, keV

Nuclide	No. of group					
	I	2	3	4	5	6
$^{232}\text{Th}_f$	$\frac{200,7}{200}$	$\frac{388,4}{370}$	$\frac{419,6}{415}$	$\frac{484,4}{495}$	$\frac{314,5}{422}$	$\frac{472,2}{550}$
$^{233}\text{U}_{th}$	$\frac{200,7}{200}$	$\frac{405,1}{383}$	$\frac{414,4}{409}$	$\frac{455,5}{467}$	$\frac{335,5}{340}$	$\frac{461,3}{440}$
$^{235}\text{U}_{th}$	$\frac{200,7}{200}$	$\frac{426,0}{417}$	$\frac{411,2}{407}$	$\frac{434,3}{453}$	$\frac{338,8}{358}$	$\frac{473,1}{509}$
$^{238}\text{U}_f$	$\frac{200,7}{200}$	$\frac{458,5}{441}$	$\frac{410,2}{404}$	$\frac{453,6}{460}$	$\frac{323,4}{445}$	$\frac{463,5}{500}$
$^{239}\text{Pu}_{th}$	$\frac{200,7}{200}$	$\frac{485,4}{470}$	$\frac{399,0}{393}$	$\frac{421,1}{434}$	$\frac{347,7}{360}$	$\frac{462,2}{470}$
$^{241}\text{Pu}_{th}$	$\frac{200,7}{200}$	$\frac{492,5}{480}$	$\frac{396,0}{390}$	$\frac{430,1}{447}$	$\frac{337,8}{415}$	$\frac{468,0}{500}$

**Note:** Numerator - data from Ref. [4]; denominator - from the present paper.

#### Measurement of reactivity and group constants of delayed neutrons.

The function  $f(t)$  as derived in the present work makes it possible to compare various systems of group constants as applied to reactivity measurement. For measuring the reactivity of reactors and critical assemblies wide use is made of the method of inverse solution of kinetics equations. The reactivity meter is inputted with the readings from a neutron flux detector, and by analogue modelling or numerical solution of the kinetics equations the reactivity  $\rho = \frac{1}{\beta_{\text{eff}}} (K-1)/K$  is calculated (where  $\beta$  is the effective proportion of delayed neutrons and  $K$  is the multiplication factor), the accuracy of determination depending on the accuracy of the delayed neutron parameters  $\{a_j, \lambda_j\}$  inputted into the reactivity meter. An error in the parameters results in a systematic instrument error. Let us consider the situation whereby in a critical reactor which has been operating for a fairly long time in a steady-state regime, the multiplication factor suddenly changes from 1 to  $K$ . We shall be interested in those values of  $K$  at which prompt neutron lifetime can be taken as  $\ell = 0$ . The kinetics equation in this case takes the form

$$\rho = 1 - \left\{ \sum_{j=1}^6 \frac{\lambda_j}{\rho} a_j [(exp - \lambda_j t) + K F_j(t)] \right\} / K n(t), \quad (3)$$

where  $F_j = \lambda_j \int_0^t n(t-\tau) \exp(-\lambda_j \tau) d\tau$ ;  $n(0) = 1$ ;  $(\gamma_j/\gamma)$  is the ratio of the value of the  $j$ -group to the group mean;  $n$  is the power. Normally, with reactivity meters it is assumed that  $(\gamma_j/\gamma) \approx 1$ , and we shall perform our calculations in this approximation.

The reactivity meter is modelled as follows. At a given reactivity, a calculation is made of the dependence of reactor power on time  $n(t)$ . The calculation is performed in a twenty-group approximation, which does not introduce any appreciable error and at the same time simplifies computation, since it makes it possible to write the relationships  $n(t)$  and  $F(t)$  in analytical form [8]. The calculated value  $n(t)$  is regarded as the detector reading delivered to the reactivity meter. By comparing the initial reactivity with the result of calculation by formula (3) using one or other set of six-group constants (reactivity meter readings), we obtained the instrument error associated with an approximate six-group description of delayed neutron properties.

The dependence of detector readings on time  $n(t)$  is determined on the basis of quantities known with finite accuracy. Therefore, simultaneously with calculation of  $n(t)$  and  $\rho$  we also calculate their possible errors. The principal contribution to the overall indeterminacy of the function  $f(t)$  is made by errors in the neutron yield from the fission fragments. Since the outputs of the various groups in a twenty-group approximation of the function  $f(t)$  are not correlated

$$D_\rho = \sum_{\ell} \left[ (d\rho/d\nu_{\ell}) \delta\nu_{\ell} \right]^2 ;$$

$$d\rho/d\nu_{\ell} = 1/n(t) \left[ (1-\rho) dn/d\nu_{\ell} - \sum_j a_j (dF_j/d\nu_{\ell}) \right] ,$$

where the index  $\ell$  denotes the twenty-group parameters used in calculating the dependence  $n(t)$ , and the index  $j$  denotes the six-group parameters inputted into the reactivity meter.

Below we give the numerical results for thermal and fast neutron  $^{235}\text{U}$  reactors. Calculations made by the authors have shown that when

measuring reactivity the dependence of delayed neutron properties on the energy of the neutrons causing fission leads to about a 3% relative difference in the reactivity meter readings (weak dependence on reactivity). This quantity is comparable with the measurement error, and hence we give the results for a fast and a thermal reactor separately.

The reactivity meter was modelled for the following four sets of six-group constants:

1. Constants derived in the present work with thermal neutron  $^{235}\text{U}$  fission;
2. The same constants with fissioning spectrum neutron fission;
3. Constants obtained [8] with thermal neutron  $^{235}\text{U}$  fission (this set is recommended in the BNAB system of constants [9]);
4. Constants derived [8] for fast neutron fission (the author recommends their use for thermal reactors also instead of set No. 3, and they are included in the ENDF/B Library [10]).

It should be pointed out that the half-life of the longest lived group  $t_{1/2} = 54.51$  s, although this group as a whole is determined by  $^{87}\text{Br}$  with  $T_{1/2} = 55.7 \pm 0.1$  s.

Figures 1, 2 show the divergence of the reactivity meter reading from its true value as a function of measurement time. The ordinate of the shaded area is equal to the possible calculational error  $\pm \sqrt{\rho/\rho}$ , associated with the imprecision in the evaluation of function  $f(t)$ .

For the six-group constants obtained in the present work, the reactivity meter readings practically coincide with the true value. This is to be expected, since both the twenty-group and the six-group constants were derived on the basis of the same data on the precursors. Hence far-reaching conclusions should not be drawn from this. It may be noted only that an increase in the number of groups beyond six is inadvisable. In the light of the  $D\rho$  value, it can be stated that this system of constants makes it possible to measure reactivity with an accuracy not poorer than  $\pm 5\%$ .



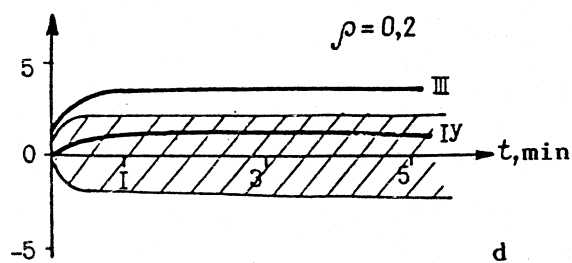
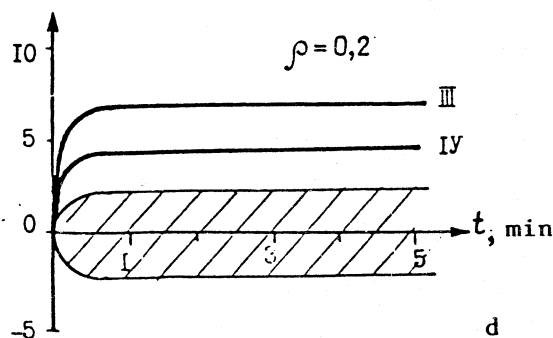
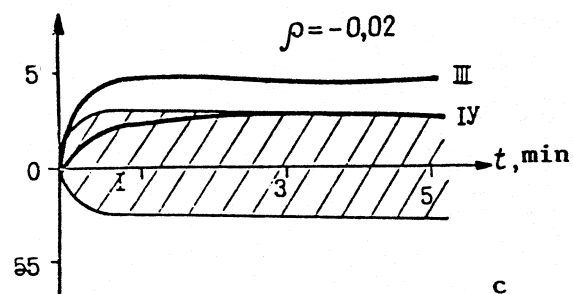
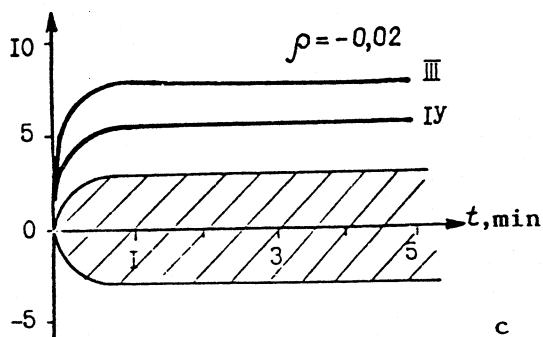
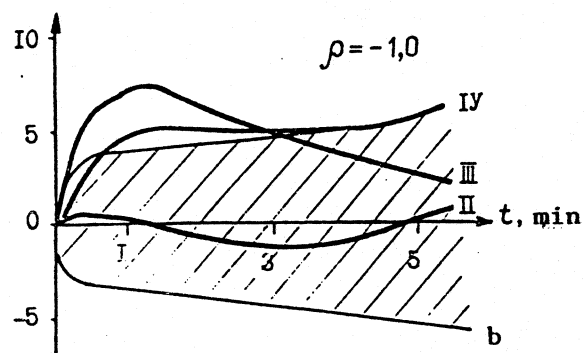
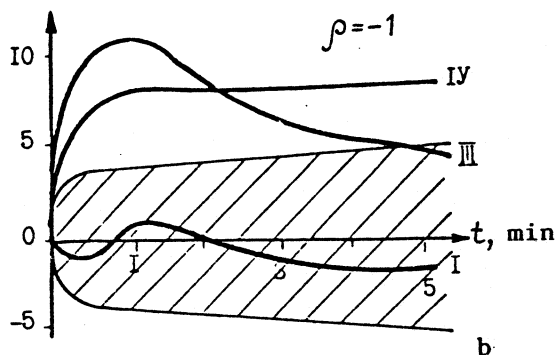
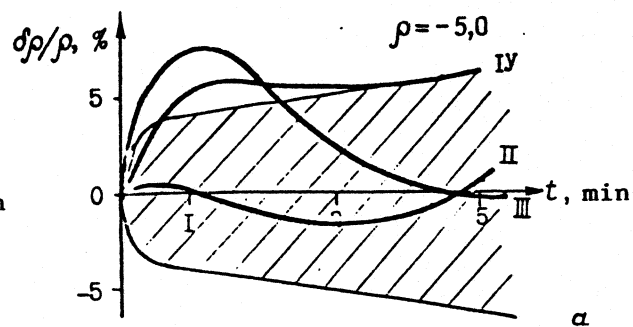
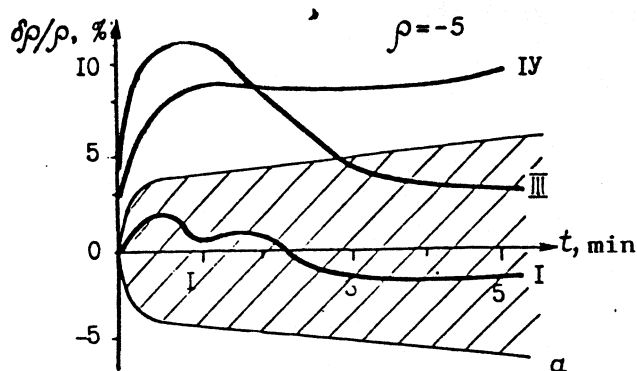


Fig. 1.

Fig. 2.

Fig. 1.

Reactivity meter error in a thermal reactor using various sets of six-group constants for various values of  $\rho$ . The figures by the curves indicate the number of the set. For variants c and d the calculational error with the constants of set No. 1 is close to zero and is not given.

Fig. 2.

Reactivity meter error in a fast reactor using various sets of six-group constants for various values of  $\rho$ . The figures by the curves indicate the number of the set. For variants c and d the calculational error with the constants of set No. 2 is close to zero and is not given.

In the case of a thermal reactor, the sets of constants Nos 3 and 4, as can be seen from Fig. 1, result in a considerable divergence (about 5-10%) of the reactivity meter reading from the true value. The difference is a function of the reactivity value and the measurement time. It would appear that thermal spectrum measurements [8] are not sufficiently accurate (the author himself does not recommend them), and use for a thermal reactor of constants derived via the fission spectrum results in appreciable error. In the case of a fast reactor (cf Fig. 2) the "error" reaches a maximum of 5-7%.

The observed discrepancy in the reactivity meter readings is the consequence of the difference in the results of measurement of the neutron activity of the decay curve by various methods: the microscopic method via the fission fragments, and the macroscopic method consisting of direct measurement. Taking a thermal reactor as example, let us see whether the results for the first and third sets of constants agree within the limits of the errors indicated by the authors. Figure 3 shows the dependence on measurement time of the reactivity meter readings with sets of constants Nos 1 and 3. The curve is the result ensuing from the microdata (set 1) assuming that the macrodata permit error-free measurements ( $\delta\rho = 0$ ). The shaded areas represent the measurement errors associated with the constant group errors (one standard deviation). In a supercritical and in a weakly subcritical reactor the results agree, but only under conditions of a sufficiently long measurement time. In a deeply subcritical reactor the results diverge, even allowing for the measurement errors.

Principal results and conclusions. The properties of delayed neutrons identified in this paper, as in Ref. [1], are compared with data recommended by other authors and used at present for the analysis of reactor kinetics. In effect this amounts to a comparison of the results of measurements of identical quantities by different methods: macroscopic and microscopic.

On the basis of evaluated data for the emitters, the neutron activity decay function  $f(t)$  is derived together with its 20-parameter representation.

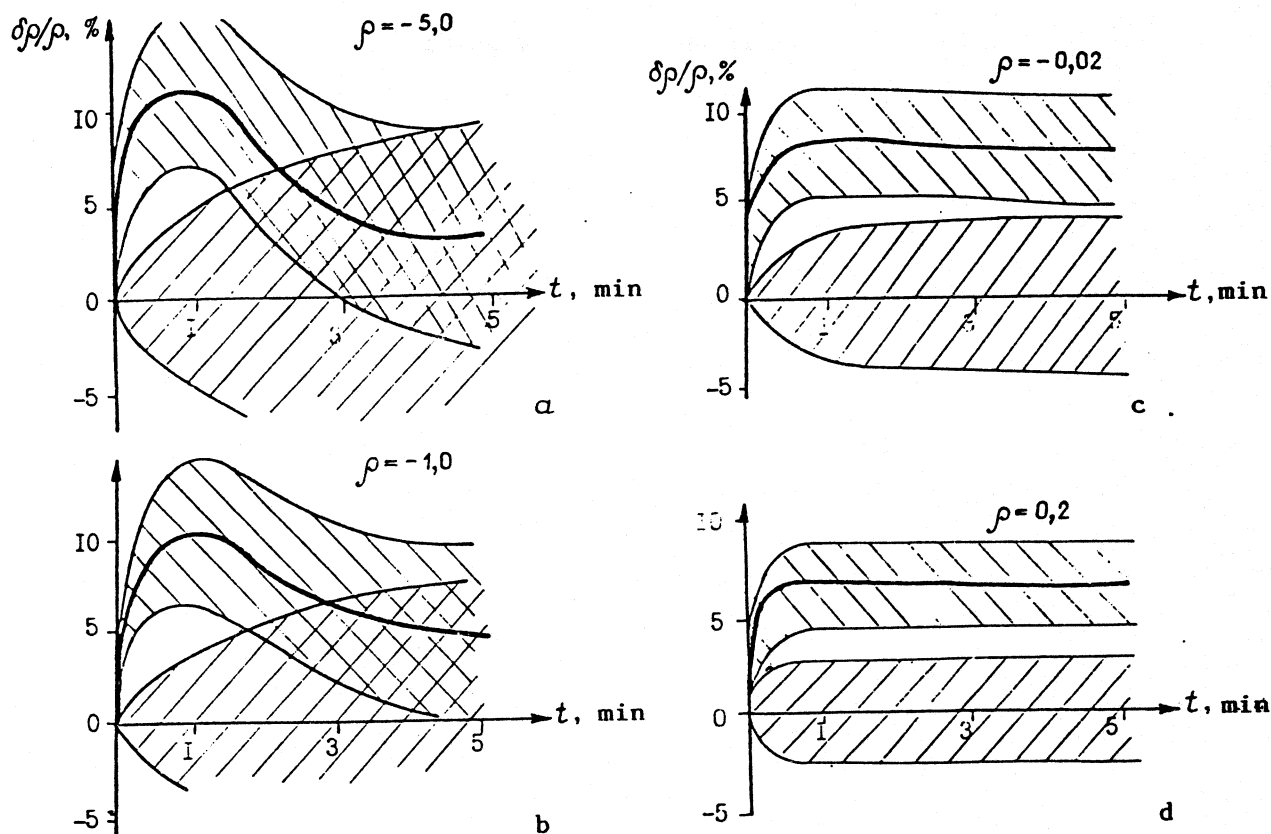


Fig. 3. Comparison of micro- and macrodata for calculations with various values of  $\rho$ .

The accuracy of the curve  $f(t)$  is determined by the size of the errors in the starting data, and for most fissionable nuclides amounts approximately to 5%. This is likewise the order of magnitude of the error in the function  $f(t)$ , established by reference to the effective six-group constants obtained on the basis of macromasurements.

The known six-group constant systems do not permit the approximation of the derived function  $f(t)$  with the necessary accuracy. In this paper we present six-group constants describing this function with minimum error. Proceeding from known experimental data and available evaluations of the mean energies for individual emitters, mean six-group energies for delayed neutrons have been derived in accordance with our breakdown of emitters by groups.

The comparison of various six-group constant systems was carried out with reference to the measurement of  $^{235}\text{U}$  reactor reactivity. The constants based on microdata make it possible to measure the reactivity with an accuracy

of 3-5%. The errors in the macroconstants lead to approximately the same degree of uncertainty. The readings of reactivity meters with micro- and macroconstants differ with any system of macroconstants. There are no decisive arguments in favour of one or other system of constants, and hence additional measurements are desirable.

#### REFERENCES

1. Manevich L.G., Nemirovskij P.Eh., Yudkevich M.S. Calculation of integral delayed neutron properties, Part 1. Total neutron yield. See present publication, 3 (in Russian).
2. Kolobashkin V.M., Rubtsov P.M., Aleksankin V.G., Ruzhanskij P.A. Beta radiation of fission products. Moscow, Atomizdat, (1978) (in Russian).
8. Keepin D.R. Physical principles and kinetics of nuclear reactors. Moscow, Atomizdat, (1967) (in Russian).
9. Abagyan L.P., Bazazyants N.O., Nikolaev M.N., Tsibulya A.M. Group constants for reactor and shielding calculations. Moscow Ehnergoizdat, (1987) (in Russian).
12. Hudson D. Statistics for physicists, Moscow, Mir, (1967) (in Russian).

[See original for other references]

Paper received by editors on 4 February 1987.

# URANIUM AND PLUTONIUM ENERGY RELEASE PER FISSION EVENT IN A NUCLEAR REACTOR

A.F. Badalov, V.I. Kopejkin

URANIUM AND PLUTONIUM ENERGY RELEASE PER FISSION EVENT IN A NUCLEAR REACTOR. The total and effective (including all contributions except those from antineutrinos and long-lived fission products) energies per fission were calculated for the nuclides  $^{235}\text{U}$ ,  $^{238}\text{U}$ ,  $^{239}\text{Pu}$  and  $^{241}\text{Pu}$ . The total thermal energy, including that from neutron capture, was derived for a WWER-440 reactor.

Consideration of heat release in the core plays an important part in solving problems of nuclear reactor safety and efficient utilization. One of the basic properties used in heat release calculations is the mean energy per fission event in the fuel nuclei. A knowledge of this quantity is also essential for determining the rate of fissions in the core when basic and applied research is being performed.

Papers have been published describing studies on fission energy (cf. [1-4] and the references therein). The most thorough investigation [1], the results of which are still widely used in the literature [5-7], was performed about 20 years ago. Some of the data on the energy release of nuclear disintegration products was derived empirically [1] and requires review. In addition, in studies [1-4] account was not taken of the dynamics of energy release associated with neutron capture in the reactor materials, and with fuel burnup and fuel reloading.

The present paper continues study [8]. Using fresh data a calculation is performed of the energy release for the principal thermal neutron reactor fuel components  $^{235}\text{U}$ ,  $^{238}\text{U}$ ,  $^{239}\text{Pu}$  and  $^{241}\text{Pu}$ . The total nuclide energy release  $E_t$  is determined, and that effective part thereof,  $E_{ef}$ , which remains in the reactor after subtraction of the energy of escaping antineutrinos  $E_\nu$  and non-disintegrating long-lived fission products  $\Delta E_{\beta\gamma}$ , and is transformed into heat:

$$E_{ef} = E_t - E_\nu - \Delta E_{\beta\gamma}. \quad (1)$$

The total thermal energy release  $E_f$  is also calculated, including, apart from the fission energy, the contribution from the capture of neutrons not participating in maintaining the chain reaction  $E_c$ :

$$E_f = E_{ef} + E_c. \quad (2)$$

Finally, calculations are performed on the total heat release  $\bar{E}_f$  per fission event for WWER-440 reactor fuel averaged as regards composition. The paper likewise considers corrections associated with delayed energy release of radioactive products, and the calculational errors are evaluated.

Total and effective fission energy. The breakdown of the nucleus gives rise to a chain of a large number of processes which occur with transformation of the fission fragments. Calculation of total energy by the "frontal" method consisting of adding together the mean energies of the individual processes leads to unjustifiably large errors, amounting to as much as 2-3 MeV [1-7]. The error is considerably reduced when calculations are performed on the basis of the relative atomic masses of the fissionable nucleus nuclides  $M(A, Z)$  and of the resulting final stable fission products  $M(A_i, Z_i)$ :

$$E_t = M(A, Z) + M_n - \sum y_i M(A_i, Z_i) - \bar{\nu} M_n, \quad (3)$$

where  $y_i$  is the fission product yield ( $A_i, Z_i$ );  $\sum y_i = 2$ ;  $M_n$  is the neutron mass;  $\bar{\nu}$  is the total neutron yield (prompt and delayed). In addition, the calculation performed in this way takes account of all possible components making up the total energy. It may be noted that the recording of this energy through the relative atomic masses (3) takes account of the mass of the  $\beta$ -particles irradiated by the fission products.

Making use of the condition of conservation of nucleon number during fission, we may rewrite expression (3) in terms of mass excess of nuclides  $m(A, Z)$ :

$$E_t = m(A, Z) - \sum y_i m(A_i, Z_i) - (\bar{\nu} - 1)m_n,$$

where  $m(A, Z) = M(A, Z) - A m_0$ ;  $m_0$  is the atomic unit of mass;

$m_n = M_n - m_0 = 8071.69 \pm 0.10$  keV is the neutron mass excess [9].

Table 1. Total and effective (1) fission energy, MeV/fission.

Nuclide	Type of fission	$m(A, Z)$	$\sum y_i m_i$	$\bar{\nu}$	$(\bar{\nu} - 1)m_n$	$E_t$	$E_\nu$	$\Delta E_{\beta\gamma}$	$E_{ef}$
$^{235}\text{U}$	Thermal neutrons	$40.93 \pm 0.010$	$-173.33 \pm 0.10$	$2.4229 \pm 0.0066$	$11.49 \pm 0.05$	$202.77 \pm 0.12$	$8.8 \pm 0.25$	0.36	$193.6 \pm 0.3$
$^{238}\text{U}$	Fissioning spectrum neutrons	$47.34 \pm 0.011$	$-173.31 \pm 0.20$	$2.81 \pm 0.03$	$14.61 \pm 0.24$	$206.04 \pm 0.31$	$11.1 \pm 0.4$	0.33	$194.6 \pm 0.5$
$^{239}\text{Pu}$	Thermal neutrons	$48.60 \pm 0.010$	$-173.65 \pm 0.20$	$2.8799 \pm 0.0090$	$15.17 \pm 0.07$	$207.08 \pm 0.21$	$7.3 \pm 0.3$	0.32	$199.5 \pm 0.4$
$^{241}\text{Pu}$	Thermal neutrons	$52.97 \pm 0.010$	$-173.70 \pm 0.30$	$2.934 \pm 0.012$	$15.61 \pm 0.10$	$211.06 \pm 0.32$	$9.2 \pm 0.4$	0.33	$201.5 \pm 0.5$

Table 1 shows the results of our calculations of total and effective energies, and likewise their individual terms. The nuclide mass excess values used in the calculation are taken from study [9] and the data on fission product yield are taken from the tables in Ref. [10], while the neutron yields are quoted from the handbook [7]. In calculating total energy, allowance is made for decay of all fission products (including the long-lived  $^{96}\text{Zr}$  and its daughter product  $^{96}\text{Nb}$ ), with the exception of  $\alpha$ -emitters. The latter have long half-lives, and the energy released by them ( $^{144}\text{Nd}$ ,  $^{147}\text{Sm}$ ,  $^{149}\text{Sm}$ ) is small and amounts to 0.14-0.17 MeV/fission event for uranium and plutonium.

The total fission energy error is governed by the imprecise knowledge of neutron yield and the error in calculating the mass excess of stable fission products  $\sum y_i m_i$ . In spite of the large number of fission products, the last-named quantity is nevertheless calculated with only a small error and hardly differs from nuclide to nuclide (see Table 1). This is brought about by the high accuracy of the mass excess data  $m_i$  and also by the fact that  $m_i$  is an almost constant quantity in the high yield ( $y_i$ ) area. As regards the error in calculating the effective energy, this is considerably more than that of the total energy, and is governed by the error in determining the energy of the escaping antineutrinos. The values for  $E_\nu$  given in Table 1 were derived by the authors by averaging data from studies performed in recent years (see [11, 12, 4] and the references therein).

Table 1 also gives our evaluations of the energy of non-decaying long-lived fission products  $\Delta E_{\beta\gamma}$  as at the end of the first year of operation of the reactor. It should be observed that this quantity is weakly dependent on fuel irradiation time. Thus, during three years' irradiation, its value drops in comparison with those given in the table by a maximum of about 0.02 MeV/fission.

A distinguishing feature of total and effective fission energy is stability vis-à-vis variations in the energy of the neutrons causing fission. In Ref. [8] it is shown that  $\Delta E_t \approx \Delta E_{ef} \approx -\Delta E_n$  when neutron energy changes within the range of 1 MeV. This means that the total and effective fission energies for a fast neutron reactor are less than those for a thermal reactor by about 0.2% at most.

Energy released during neutron capture by reactor materials. From the number  $\bar{\nu}$  of neutrons emitted on average per fission event, only one participates in maintaining the chain reaction leading to the emission of about 200 MeV of energy. On capture of the remaining  $(\bar{\nu} - 1)$  neutrons the energy release represents about 5% of that liberated on fission. However, unlike fragments and  $\beta$ -particles, neutrons are capable of penetrating for great distances from the point of nuclear fission. After they have been moderated they are effectively captured by numerous structural components. In the case of some of them, the energy release from neutron capture predominates and its calculation requires special attention.

Below we present a calculation which we have made of the contribution to heat release accruing from capture, in respect of the principal neutron absorbers. The calculation covered both the energy of the capture reaction [essentially  $(n,\gamma)$ ], as a direct operation, and the subsequent radioactive transformations of the daughter nucleus, with subtraction of the antineutrino and long-lived product energy. The energy associated on average with each neutron capture event in reactor materials, in MeV/neutr., is as follows:  $^{235}\text{U} - 6.55$ ;  $^{238}\text{U} - 5.70$ ;  $^{239}\text{Pu} - 6.53$ ;  $^{240}\text{Pu} - 5.25$ ;



$^{241}\text{Pu}$  - 6.30;  $^{10}\text{B}$  - 2.79; zirconium - 8.07;  $^{135}\text{Xe}$  - 7.99;  $^{149}\text{Sm}$  - 7.99;  
fission products - 8.0; hydrogen - 2.2.

Calculation of the mean heat release from the capture of a single neutron  $E_{nc}$  requires a knowledge of the neutron balance. This calculation was carried out using the UNIRASOS [13] program for several initial WWER-440 reactor campaigns.

The proportion of captures effected by the principal neutron absorber - the nuclide  $^{238}\text{U}$  - changes only insignificantly during the campaign. The same applies to the joint contribution of  $^{235}\text{U}$  and  $^{239}\text{Pu}$ , which in addition have almost identical capture energies. The total contribution of uranium and plutonium makes up two-thirds of all captures. The proportion of captures by structural materials and water likewise undergoes practically no change and accounts for a few per cent. The above reactor materials make a contribution to the constant component of energy release during capture. The dynamics of energy release  $\bar{E}_{nc}$  is governed by the absorption of neutrons in boron and fission products.

Figure 1 shows a graph for the growth of energy release during neutron capture  $\bar{E}_{nc}$  for a WWER-440 reactor during the first four runs before coming onto a steady-state regime. The growth of  $\bar{E}_{nc}$  both during the course of each campaign (continuous line) and as a whole over the first few campaigns is governed by a reduction in neutron captures in boron and an increase in fission products. With the reactor operating in a steady-state regime the quantity  $\bar{E}_{nc}$  increases during the campaign from 5.6 to 6.0 MeV/neutr. The error in its determination amounts to  $\pm 0.2$  MeV/neutr.

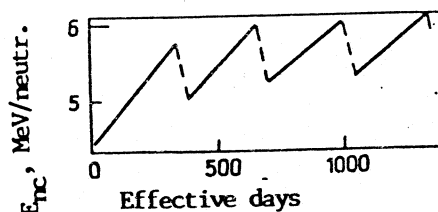


**Fig. 1.** Energy release (continuous line) during neutron capture without fission in the course of the four first campaigns of a WWER-440 reactor (the dotted line represents reactor refuelling).

Total thermal energy per fission. This value includes all forms of thermal release in the reactor over the entire cycle of transformation of the fissionable nucleus and its fragments. It is determined by expression (2) and can be rewritten in the form  $E_f = E_{ef} + (\bar{\nu}-1)\bar{E}_{nc}$ , where  $E_c = (\bar{\nu}-1)\bar{E}_{nc}$  is the energy from neutron capture per fission event.

Table 2. Total thermal energy released in a thermal neutron reactor and its components from fission and capture of neutrons, MeV/fission.

Nuclide	$E_{ef}$	$(\bar{\nu}-1)\bar{E}_{nc}$	$E_f$
$^{235}\text{U}$	193,6 $\pm$ 0,3	8,2 $\pm$ 0,4	201,8 $\pm$ 0,5
$^{238}\text{U}$	194,6 $\pm$ 0,5	10,5 $\pm$ 0,5	205,1 $\pm$ 0,7
$^{239}\text{Pu}$	199,5 $\pm$ 0,4	10,9 $\pm$ 0,5	210,4 $\pm$ 0,6
$^{241}\text{Pu}$	201,5 $\pm$ 0,5	11,2 $\pm$ 0,5	212,7 $\pm$ 0,7

Table 2 shows the energies  $E_f$  as calculated by the authors for the principal components of reactor fuel,  $^{235}\text{U}$ ,  $^{238}\text{U}$ ,  $^{239}\text{Pu}$  and  $^{241}\text{Pu}$ .

Here the energy release from neutron capture was taken as

$\bar{E}_{nc} = 5.8 \pm 0.2$  MeV/fission, which corresponds to the middle of a steady-state reactor campaign. By introducing proportions  $\alpha^i$  of uranium and plutonium (in terms of fissions), it is possible to determine the energy  $\bar{E}_f = \sum \alpha^i E_f^i$ , averaged in respect of the fuel composition, where the indices  $i$ , equal to 5, 8, 9, 1, relate to the above-enumerated nuclides (Table 3). It is considered [14] that the error in determining the contribution  $\alpha^i$  is 10% (relative). On this basis, it is possible to evaluate the additional error introduced into the calculation of  $\bar{E}_f$  (0.5 MeV/fission).

The slow nature of the  $\beta$ -decay process of fission products also has an effect on the dynamics of energy release in the reactor. The delay in  $\beta$ -decay relative to the instant of fission results in a delay in the release of a portion of the energy after reactor startup, during transition from one power level to another and upon shutdown.

Table 3. Contributions of  $\alpha^i$  of the nuclides  $^{235}\text{U}$ ,  $^{238}\text{U}$ ,  $^{239}\text{Pu}$ ,  $^{241}\text{Pu}$  in terms of number of fissions and total thermal energy release  $\bar{E}_f$  averaged over the fuel composition for three WWER-440 reactor campaigns.

Reactor campaign	$\alpha^5$	$\alpha^8$	$\alpha^9$	$\alpha^1$	$\bar{E}_f$ , MeV/fission
First	$\frac{0,861^*}{0,526}$	$\frac{0,071}{0,078}$	$\frac{0,068}{0,355}$	$\frac{0}{0,041}$	$\frac{201,7^{*2}}{205,5}$
Second	$\frac{0,681}{0,486}$	$\frac{0,073}{0,078}$	$\frac{0,223}{0,370}$	$\frac{0,023}{0,066}$	$\frac{203,8}{206,3}$
Third	$\frac{0,707}{0,513}$	$\frac{0,073}{0,077}$	$\frac{0,197}{0,348}$	$\frac{0,023}{0,062}$	$\frac{203,8}{206,1}$

- \* The numerator always contains the values for the start of the campaign and the denominator the values for its end.
- \*\* Allowance here made for the fact that after one month's reactor operation the energy of the non-decaying long-lived fission products amounts to 0.55 MeV/fission.

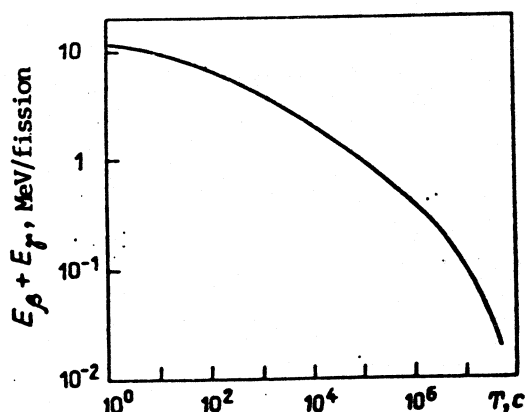


Fig. 2. Residual heat release in a WWER-440 reactor after a year's irradiation of the fuel.

The dependence of the residual energy released with  $\beta$ -decayed-associated  $\beta$ -particles and  $\gamma$ -photons on the holding time of the fuel after a year's irradiation is shown in Fig. 2. The initial data for calculating this dependence are taken from Refs [4, 15]. It will be seen that one month after reactor shutdown the residual heat release constitutes about 0.25 MeV/fission, and two months later it amounts to 0.16 MeV/fission. The fall in activity with time slows down, and after four months the heat release still amounts to 0.1 MeV/fission. These corrections to the residual heat release must be taken into account in calculating the value  $\bar{E}_f$ .

The authors associate a further reduction of the error in calculating energy release with a refinement of the value for the energy removed by antineutrinos, with making careful allowance for the neutron balance and with more accurate calculation of the contributions in terms of number of fissions of fuel nuclei for each specific reactor.

The authors wish to express their warm thanks to M.A. Mikaelyan for useful discussions.

#### REFERENCES

1. James M.F., Energy released in fission. J. Nucl. Energy 23 9 (1969) 517-536.
2. James M.F., The useful energy released in the fission of  $^{232}\text{Th}$ ,  $^{233}\text{U}$ ,  $^{234}\text{U}$ ,  $^{236}\text{U}$ ,  $^{237}\text{Np}$ ,  $^{238}\text{Pu}$ ,  $^{240}\text{Pu}$ ,  $^{242}\text{Pu}$ . Ibid. 25 10 (1971) 517-521.
3. Nemirovskij P.Eh., Manevich L.G., Fission energy of isotopes of uranium and transuranic elements, Vopr. atom. nauk i tekhn. Ser. Yad. Konst. 5 (1981) 3-9. (in Russian).
4. Tasaka K., Ihara H., Akiyama M. INDC nuclear data library of fission products. Preprint 12871 Japan Atomic Energy Research Institute (1983).
5. Glushkov E.S., Demin V.E., Ponomarev-Stepnoj N.N., Khrulev A.A., Heat release in a nuclear reactor, Moscow, Ehnergoatomizdat (1985) (in Russian).
6. Kolobashkin V.M., Rubtsov P.M., Ruzhanskij P.A. et al., Radiation properties of irradiated nuclear fuel, Moscow, Ehnergoatomizdat (1983) (in Russian).
7. Gorbachev V.M., Zamyatin Yu.S., Lbov A.A., The interaction of radiations with heavy-element nuclei and nuclear fission, Moscow, Atomizdat, (1976) (in Russian).
8. Kopejkin V.I., Energy released per uranium and plutonium fission event in a nuclear reactor: IAEh Preprint 4305/2, Moscow (1986) (in Russian).
9. Kravtsov V.A., Atomic masses and nuclear binding energies, Moscow, Atomizdat (1974) (in Russian).
10. Crouch E.A.C., Fission-product yields. Atomic Data Nucl. Tables. 19 (1977) 419-509.
11. Vogel P., Schenter G.K., Mann F.M., Schenter R.E., Reactor antineutrino spectra and their application to antineutrino-induced reactions. Phys. Rev. C24 (1981) 1543-1555.
12. Dickens J.K., Electron antineutrino spectrum for  $^{235}\text{U}(n,f)$ . Phys. Rev. Letters 46 (1981) 1061-1064.

13. Sidorenko V.D., Pshenin V.V., Engineering methods and programs for preparing small-group constants for calculations of cores with light-water moderators, Vopr. atom. nauk. i tekhn. Ser. Fiz. i tekhn. yad. reaktorov, 4 (1985) 3-9 (in Russian).
14. Korovkin V.A., Kodanov S.A., Yarichin, A.D. et al., Measurement of nuclear fuel burnup in a reactor by reference to neutron radiation At. Energiya. Vol. 156 (1984) 214-218 (in Russian).
15. Ovchinnikov F.Ya., Golubev L.I., Dobrynin V.D. et al., Operating regimes of water moderated and cooled nuclear power reactors, Moscow, Atomizdat (1979) (in Russian).

Paper received by editors on 12 August 1987.



# THE USE OF EVALUATED NUCLEAR DATA LIBRARIES FOR THE CALCULATION OF KERMA FACTORS

I.M. Bondarenko, A.S. Zabrodskaya, A.S. Krivtsov, I.N. Nikolaev

**CALCULATION OF KERMA FACTORS USING EVALUATED NUCLEAR DATA LIBRARIES.**  
A computational model is developed for calculating neutron kerma factors and total energy of protons from basic nuclear data for all neutron reaction types in any energy range. The evaluated nuclear data libraries are used for calculating the kerma factors.

In the design of any nuclear power facility, much importance is attached to calculating heat release in all sections of the facility. For calculating heat release as a result of the interaction of neutrons with matter, use is usually made of kerma (kinetic energy released in materials) factors [1, 2], determined in the following manner:

$$K(E) = \sum_i \sigma_i(E) / E_{Hi}(E),$$

where  $K(E)$  is in b·eV/atom;  $\sigma_i(E)$  is the microscopic cross-section for a nuclide in the  $i$ -th reaction for neutron energy  $E$ ;  $E_{Hi}(E)$  is the energy released locally in the  $i$ -th reaction.

If the neutron fluxes and the kerma factors are known, the heat release from the neutrons can be easily calculated [2]. In calculating the energy release in steady-state facilities, the energy  $E_{Hi}$  must include not only the prompt but also the delayed release of energy from the decay of neutron reaction products (if the half-life is less than three years). Sometimes, in calculating a reactor core, account is not taken of energy transport by photons, implying local absorption of photons at the place of their formation. In this case the energy of the photons formed in the  $i$ -th reaction must also be included in the energy  $E_{Hi}$ . The energy  $E_{Hi}$  will denote the total energy release in the  $i$ -th neutron reaction. Since neutron fluxes are generally obtained in a multigroup approximation, so the kerma factors must be averaged by groups:  $K^g = \sum_i \sigma_i^g E_{Hi}^g = \sigma_{el}^g E_{el}^g f_{el}^g + \sigma_{in}^g E_{in}^g + \sigma_c^g E_c^g f_c^g + \sigma_f^g E_f^g f_f^g$ , where

[\*] Paper presented at the International Conference on Neutron Physics, Kiev, 14-18 September 1987.

$E_{el}^g$ ,  $E_{in}^g$ ,  $E_c^g$  and  $E_f^g$  is the average energy released in group  $g$  from elastic scattering of neutrons, and also from inelastic scattering of neutrons, capture neutrons and fission neutrons, respectively (averaging is carried out in energy group  $g$  with the weight of the corresponding cross-section). Here account is taken of the fact that the group cross-sections can depend in large measure on the composition of the medium as a result of resonance self-shielding. In this expression, the self-shielding effect is taken into account explicitly by means of the customarily-used factors [3].

Locally released energy for the first three types of reaction are calculated in the following manner [1, 2]. The mean energy of the recoil nucleus in elastic scattering of neutrons is equal to  $E_{el}(E) = [1 - \bar{\mu}_{el}(E)] 2AE/(1+A)^2$ , where  $\bar{\mu}_{el}(E)$  is the mean cosine of the neutron elastic scattering angle in a centre-of-mass system;  $A$  is the ratio of the mass of the nuclide nucleus to the mass of the neutron. For inelastic neutron scattering

$$E_{in}(E) = \sum_i \sigma_{in,L}(E)/\sigma_{in}(E) [E - \bar{E}_{n',L} - E_{\lambda,L}/(1+C_{F,L})] + \\ + \sigma_{in,cont}(E)/\sigma_{in}(E) (E - \bar{E}_{n',cont} - \bar{E}_{cont}) + \sum_z \sigma_{in,z}(E)/\sigma_{in}(E) (E - \bar{E}_{n',z} + Q_z - \bar{E}_z + \bar{E}_{dz}),$$

where  $\bar{E}_{n',r}$  is the mean energy of the emitted neutron (neutrons) in reaction  $r$ ;  $E_{\lambda,L}$  is the excitation of discrete level  $L$ ;  $Q$  is the energy of the reaction;  $\bar{E}$  is the mean excitation energy of the residual nucleus;  $C_F$  is the internal conversion coefficient;  $\bar{E}_d$  is the mean  $\beta$ -particle energy.

The first term of the sum takes account of inelastic neutron scattering with excitation of discrete levels, the second term with excitation of a continuum of levels, and the third term with emission of charged particles, the reactions  $(n,2n')$ ,  $(n,3n')$  etc. (in these cases  $\bar{E}_{n'}$  is the mean energy of two or, as the case may be, three neutrons). The mean kinetic energy of a neutron emitted in the laboratory system of co-ordinates in inelastic scattering at level  $L$  is equal to

$$\bar{E}_{n',L} = \left[ \frac{A^2+1}{2A} - \frac{1+A}{2} \frac{E_{\lambda,L}}{E} + \left( 1 - \frac{A+1}{A} \frac{E_{\lambda,L}}{E} \right)^{1/2} \bar{\mu}_L(E) \right] \frac{2AE}{(1+A)^2},$$



where  $\bar{\mu}_L(E)$  is the mean cosine of the scattering angle in a centre-of-mass system. The value  $\bar{\epsilon}_{\text{const}}$  is linked to the expression  $\bar{\epsilon}_{\text{cont}} = \frac{A^2+1}{A(A+1)} - \frac{A+1}{A} \bar{\epsilon}_{n',\text{cont}}$ .

For neutron inelastic scattering reactions with the emission of charged particles, when the files contained no information on the excitation of individual residual-nucleus levels, the energy was taken as  $\bar{\epsilon}_r = 0$ , and for the  $(n,2n')$  reaction this energy was calculated in terms of the mean energies of each neutron emitted:

$$\bar{\epsilon} = \frac{A^2+2}{A(A+1)} E - |Q| - \frac{1}{A-1} \left( \frac{A^2-2}{A} \bar{\epsilon}_{n'_1} + A \bar{\epsilon}_{n'_2} \right).$$

For reactions leading to the adsorption of a neutron (without fission),

$$E_c(E) = \frac{\sigma_{n,\gamma}(E)}{\sigma_c(E)} \left\{ \frac{E}{A+1} + \frac{[Q_{n\gamma} + AE/(A+1)]^2}{2M_r C^2} \right\} + \sum_i \sum_j \frac{\sigma_{ij}(E)}{\sigma_c(E)} (E + Q_i - \epsilon_{ij} + \bar{E}_{d,ij}),$$

where  $M_r C^2$  is the residual-nucleus mass in energy units, and  $M_r C^2 = (A+1)m_n C^2 - Q_{n\gamma}$  (where  $m_n C^2 = 939.55$  MeV). The first term takes into account radiative capture, and the second covers the sum of reactions with formation of charged particles, when a residual nucleus is in the  $j$ -th excited state. For the fission reaction, the mean locally-emitted energy is equal to the mean kinetic energy of the fission fragments plus the mean  $\beta$ -particle energy from fission product decay.

For calculating group neutron kerma factors, the following libraries of evaluated neutron data were used: ENDF/B.IV, ENDL-83, JENDL-2. Necessary information about radioactive decay of fission products was taken from Ref. [4]. Where there was no such information available for certain decaying nuclides, the mean kinetic energy of  $\beta$ -particles was determined by the procedure used in Ref. [2]. In addition to the local release of energy, the total release was also calculated for all types of reaction. The difference between these values gives the total energy of photons produced in these reactions. It may be noted that this value often differed substantially from that following from the evaluated data on proton formation cited for the same

nuclide. Thus, the energy balance in the reactions is not always established in the evaluated data libraries.

In the fission reaction, account was taken both of the energy of prompt fission protons and of the energy of delayed photons from  $\beta$ -decay of fission products with a half-life up to three years.

Since there are no nuclide-by-nuclide files for some elements, it was not possible to perform an exact calculation of their kerma factors. In these cases, the contribution of the individual nuclides to the total kerma factor for an element was evaluated from additional information on thermal neutron capture cross-sections, resonance integrals, mean cross-sections for threshold reactions over the fission spectrum and with allowance for their percentage content.

Energy release in neutron reactions with 13-A1-27													
NC	E-EL MEV	E-C MEV	E-IN MEV	KERMA-S MEV*3	PERCENT			T-C MEV	T-IN MEV	TERMA-S MEV*3	PERCENT		
					E	C	IN				E	C	IN
1	5.82-1	11.710	1.721	4.42-2	4	68	36	14.26	6.168	9.873	2	36	62
2	2.78-1	9.406	2.861	3.28-2	6	69	25	11.94	3.354	7.523	2	35	63
3	2.32-1	6.445	2.373	1.18-2	10	56	26	7.98	4.303	4.635	5	18	77
4	1.59-1	3.718	2.240	4.97-1	45	18	37	4.76	2.611	2.319	10	5	85
5	1.17-1	1.978	2.148	3.37-1	74	2	24	3.26	1.821	1.244	70	1	79
6	0.16-2	1.305	2.495	2.49-1	89	2	11	11.52	1.205	0.535	41	0	59
7	5.12-2	1.280	2.032	1.71-1	98	2	2	11.14	0.963	0.245	43	1	31
8	3.22-2	1.263	2.0	1.38-1	100	0	0	10.87	0.2	0.135	56	4	2
9	1.06-2	1.252	2.0	7.19-2	99	1	2	12.78	0.2	0.288	59	11	0
10	9.86-3	1.247	2.0	5.38-2	95	5	2	12.76	0.2	0.274	70	32	2
11	4.85-3	1.245	2.0	2.75-2	92	8	2	12.75	0.2	0.245	56	44	2
12	2.25-3	1.243	2.0	2.51-2	61	39	2	12.75	0.2	0.182	15	95	2
13	1.84-3	1.243	2.0	4.89-3	23	77	2	10.75	0.2	0.034	3	97	2
14	4.85-4	1.242		1.99-2	4	96		10.75		0.166	1	99	
15	2.25-4	1.242		5.28-3	6	94		10.75		0.043	1	99	
16	1.84-4	1.242		2.97-3	5	95		10.75		0.025	1	99	
17	4.85-5	1.242		2.68-3	3	97		10.75		0.022	0	100	
18	2.25-5	1.242		3.25-3	1	99		10.75		0.028	0	100	
19	1.84-5	1.242		4.18-3	2	100		10.75		0.035	0	100	
20	4.85-6	1.242		5.61-3	0	100		10.75		0.049	0	100	
21	2.25-6	1.242		0.74-3	2	100		12.75		0.271	2	100	
22	1.84-6	1.242		1.21-2	0	100		12.75		0.185	2	100	
23	4.85-7	1.242		1.78-2	0	100		12.75		0.154	0	100	
24	2.25-7	1.242		2.61-2	0	100		12.75		0.226	0	100	
25	1.84-7	1.242		3.82-2	2	100		12.75		0.331	2	100	
26	4.85-8	1.242		5.61-2	0	100		12.75		0.485	0	100	
27	2.25-8	1.242		0.74-2	0	100		12.75		0.713	0	100	
28	1.76-9	1.242		2.92-1	0	100		12.75		2.506	0	100	

With allowance for energy release in the decay of radio-nuclides formed in neutron reactions

Process	Reaction	Group	Product	T = 1/2	E <sub>p</sub> , MeV	E <sub>γ</sub> , MeV
Capture	122	-1126	AL-28	2.24 min	1.741	1.779
	123	-114	MC-27	9.46 min	0.782	0.894
	127	-113	KA-24	15.01 h	2.553	4.171

Note: KERMA-S: total kerma factors for elastic and inelastic scattering and capture; TERMA-S: total kerma factors with allowance for absorption of photons for the same reactions.

The procedure described above was used, for 114 nuclides and elements including 28 actinides, to calculate the local and total energy release from elastic and inelastic scattering of capture and fission neutrons, and also their kerma factors. The information obtained is available at the Nuclear Data Centre (Obninsk). The table shows the results for  $^{27}\text{Al}$ .

#### REFERENCES

- [1] ABDON, M.A., MAYNARD, C.W., Nucl. Sci. and Engng. 56 (1975) 360.
- [2] BONDARENKO, I.M., Kerma factors in the interaction of neutrons with lithium hydride. Vopr. atom. nauk i tekhn. Ser. Yad. Konst. No. 4(31) (1978) 83 (in Russian).
- [3] ABAGYAN, L.P., BAZAZYANTS, N.D., BONDARENKO, I.I., NIKOLAEV, M.N., Group constants for calculating nuclear reactors, Moscow, Atomizdat (1964) (in Russian).
- [4] POPOV, V.I., MOISEEVA, A.A., Radionuclide decay schemes. Radiation energy and intensity, Moscow, Energoatomizdat (1987) (in Russian).

Paper received by editors on 28 January 1988.



## TARGET PROPERTIES AND NUCLEAR DATA

N.V. Kornilov, A.A. Goverdovskij

TARGET PROPERTIES AND NUCLEAR DATA. The influence of the properties of the target on nuclear data was shown. In the case of targets consisting of fissionable material, this influence was demonstrated in experiments involving fission cross-section, average number of neutrons, and prompt fission neutron spectrum. The experimental methods for determining certain corrections was analysed. The method of tritium density determination for a solid target used as neutron source was likewise demonstrated.

The need for high accuracy in deriving nuclear data makes stringent demands on experimental techniques, including study of the effect of target and sample properties on experimental results. Such properties as the number of nuclei in the sample, the nuclide composition, the homogeneity of the layer through its thickness, and the non-homogeneity of the surface may exercise an unexpected effect on experimental results. Below we present cases of this effect, and also a number of ways of allowing for it, taking as examples targets consisting of fissionable materials and targets serving as neutron sources. The effects shown are considered from the point of view of the user, for whom it is of paramount importance to understand the nature of the phenomenon and to determine methods of introducing the necessary corrections to his final results.

Targets consisting of fissionable materials. Fission fragment recording efficiency, which is to a considerable extent governed by the homogeneity of the layer, has a direct influence on measurement of such quantities as fission cross-section. The effect of this property of the layer when measuring the number of prompt neutrons is more indirect and ambiguous.

In Ref. [1] this effect was studied using layers of  $^{238}\text{U}_3\text{O}_8$  with the addition of a certain quantity of  $^{252}\text{Cf}$ . Knowledge of the  $^{252}\text{Cf}$  activity made it possible to determine with sufficient accuracy (about 2%) the efficiency of fragment recording. A study was made of the dependence  $\eta = v/v_0$  (where  $v$ ,  $v_0$  is the recorded and the actual

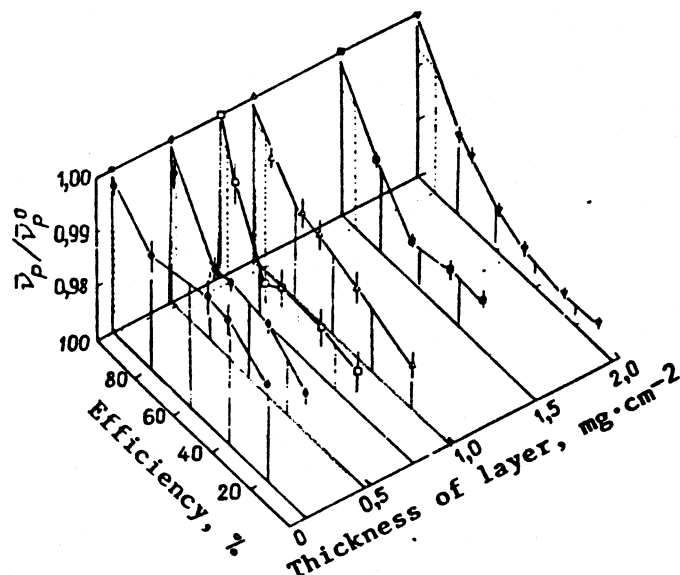


**Fig. 1.** Recorded number of prompt fission neutrons as a function of fragment recording efficiency and layer thickness, according to Ref. [1].

number of secondary neutrons) on recording efficiency and thickness of layer (Fig. 1). In addition the quantity  $\delta$  was derived, characterizing the number of events as a result of self-absorption in the layer, equal to  $1 - \eta$  (at  $E = 0$ ). The authors interpret the results obtained as follows. The greatest change in the quantity  $\eta$  occurs with a change in efficiency from 100 to 70%, when it would appear that fission events with low kinetic energy and high  $\nu$  are lost.

Discrimination of fragments and losses in the layer also lead to a strong dependence of the number  $\nu$  on the angle relative to the normal to the layer. Reference [2] contains a study on  $^{238}\text{U}$  fission neutron spectra for initial neutron energies of 6-14 MeV. Use was made of a multi-layer ionization chamber with layers of  $1.5 \text{ mg/cm}^2$  thickness. The fragment recording efficiency attained 75-80%. The layers were arranged parallel to the incident neutron flux, so that at an angle of neutron escape of  $90^\circ$  the direction to the neutron detector coincided with the perpendicular to the layer. The derived values of  $\nu(\theta)$  are shown in Fig. 2. The appreciable angular dependence (about 15%) may be associated with the following effect. As a result of non-recording (self-absorption, discrimination threshold),

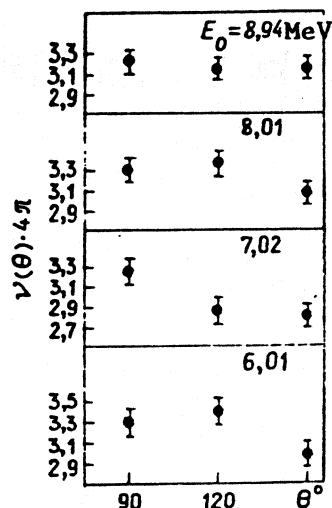


**Fig. 2.** Number of prompt neutrons recorded at a given angle relative to the incident beam.

those fragments are lost which escape essentially along the layer and emit the smallest number of neutrons in the direction  $\theta = 90^\circ$ . However, in all probability this is not the only cause, as is indicated by the change in the nature of the dependence on initial energy. With strong variation in the value  $\nu(\theta)$ , the change in the shape of the spectrum is slight. Thus, when  $E_0 \approx 7$  MeV  $T(150^\circ)/T(90^\circ) = 1.026$ , where  $T$  is a parameter characterizing a Maxwellian neutron distribution.

For measuring the ratios of the fission cross-sections of a nuclide under investigation, for example  $^{235}\text{U}$ , the threshold cross-section method [3] is a promising approach to the problem of absolute measurement of the number of nuclei in the layer and of recording efficiencies. The limitations of the method are associated with the possibility of thermal neutron fission of the nuclide under investigation.

In Ref. [4] the method was applied to the measurement of the fission cross-section ratios of  $^{237}\text{Np}$  and  $^{235}\text{U}$ . Use was made of seven targets with varying  $^{235}\text{U}$  contents (3.4–35%). No dependence of the cross-section ratios on  $^{235}\text{U}$  concentration was detected. The accuracy of measurement of the cross-section ratio was about 2.5%. The methodological difficulty lay in securing the homogeneity of layers of mixtures with a thickness of about

200  $\mu\text{g}/\text{cm}^2$ . Measurement of the fragment spectra occurring upon thermal and fast neutron fission at various angles to the perpendicular showed that there are no significant inhomogeneities in the  $^{235}\text{U}$  concentration. This kind of test, although it does not represent a direct method of measuring the concentration of a mixed nuclide, can nevertheless be useful in determining homogeneity in other experiments also.

Fragment losses as a result of self-absorption in the layer, taking account of angular anisotropy, can be determined in the way proposed in Ref. [5], although the formulae quoted below differ from those obtained in this work. For various orientations of the layers relative to the incident beam they take the form

$$\begin{aligned} I_0(t) &= \left(\frac{t}{R} - \eta\right)^2 \frac{R}{2t} \left(1 - \frac{a_2}{2}\right); \\ I_{\pi}(t) &= \left(\frac{t}{2R} + \eta\right) \left(1 - \frac{a_2}{2}\right); \\ \eta &= \left(A_f \frac{E_n}{T_f}\right)^{1/2} / (A+1) \approx 0,005 \sqrt{E_n}. \end{aligned} \quad (1)$$

In deriving these formulae the main significance attaches to the proposition regarding homogeneity of the surface and the plane-parallelism of the layer. Efficiency is affected not only by the layer thickness  $t$  and the mean range of the fragments  $R$ , but also by the inhomogeneity of the layer, its porosity and the presence of crystallization centres. Hence it is advisable to study the dependence of recording efficiency  $\epsilon = 1 - I$  on the relationship  $t/R$ .

In an investigation of this kind Ref. [6], determining the mean range  $R$  for a specific layer structure, the effect of layer inhomogeneity on the quantity  $\epsilon$  was stressed. However, the dependence of  $\epsilon$  on incident neutron energy and anisotropy was not tested experimentally. Let us consider the possibilities of such studies. The effect of these factors is small (2-3%), and therefore it makes sense to consider relative experiments. For example, measurement of the ratio of efficiencies of layers of equal thickness:



$$\alpha = (1 - I_0)/(1 - I_{\eta}) \quad (2)$$

If both the correlations (1) are correct, we should observe a substantial growth in the quantity  $\alpha$  from neutron energy with a weak dependence on target thickness (see table). The slight variation in the number of nuclei is not significant, since this results in a shift of the dependence towards a constant quantity.

Dependence of  $\alpha$  on energy for an isotropic angular distribution.

$E_n$ , MeV	$t/R=10^{-2}$	$t/R=10^{-1}$
4	1,015	1,021
8	1,020	1,029
12	1,023	1,036
16	1,026	1,041
20	1,028	1,045

It will be useful to consider the joint effect of the kinematic factor and angular distribution. Such investigations can be carried out as follows. If we place in a fission chamber two targets, prepared in the same way and from the same material, for example  $^{235}\text{U}$ , and measure the ratio of the fission fragment counting rates from these targets  $S(E)$ , then where  $t_1 \ll t_2$  the energy dependence  $S(E)$  will be a direct reflection of the change in the fragment recording efficiency in the second target. Measurements made by the time-of-flight method with a "white" neutron source are the most effective.

Figure 3 shows the expected energy dependence  $I_2(E_n)$  for a thick  $^{235}\text{U}$  target  $L/R = 0.25$  ( $t = 1.2 \text{ mg/cm}^2$ ). It will be seen from the figure that the dependence  $I_2(E_n)$  undergoes changes of over 3% in the range of  $E_n$  from thermal to about 9 MeV. The "steps" in the energy dependence are associated with variation in the fission fragment angular distributions. The dotted curve indicates the change in  $I_0$  as a result of variation only of the kinematic factor  $\eta$ . On the basis of experimental data it would be possible not only to check the correctness of formula (1) but also to determine (as a

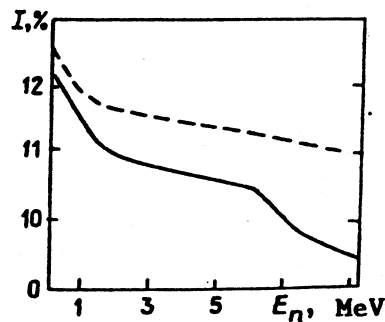


**Fig. 3.** Proportion of lost fragments  $I_0$  depending on initial neutron energy for a  $^{235}\text{U}$  target of thickness  $t/R = 0.25$ ;  
 - - - - changes in  $I_0$  with an isotropic distribution.

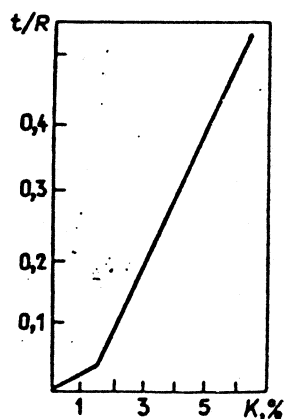


**Fig. 4.** Dependence of the parameter  $t/R$  on the measured ratio  $K$ .

unique parameter) the value of  $t/R$ . This parameter can be determined by another method also, which can be applied in experiments with monoenergetic neutrons. For example, it is sufficient to determine the ratio

$K = S(E_n = 9 \text{ MeV})/S(E_n = \text{therm})$  (the energy 9 MeV was chosen arbitrarily), and on the basis of the anticipated dependence (Fig. 4)  $t/R(K)$  to determine the parameter  $t/R$ . The accuracy of such an approach is governed by the derived function shown in Fig. 4, and by the measurement error  $K(\delta K/K \approx 0.2-0.4\%)$ .

For checking the layer thickness  $t$  we may recommend a quite convenient fission fragment spectrometry method using a semiconductor counter [7]. By altering the angle between the perpendicular to the layer and the direction towards the detector, it is possible to measure the value of  $t$  in energy units. It is apparently feasible to treat systematically the amount of energy

lost in the layer. The method proposed in Ref. [6] for determining fragment recording efficiency is complex and cannot be widely applied. In this connection it would be useful to study and prepare systematics for the dependence of  $\epsilon$  on the ratio between the counting rates at the curve minimum (low amplitudes) and the maximum of the fission fragment spectrum. These data can be widely used likewise in the laboratories of developing countries.

The effect of the target parameters on fission cross-section measurement results can be illustrated by two examples. Let us note here that another treatment of the results, different from ours, is possible.

$^{237}\text{Np}$  fission cross-section. In the neutron energy range  $E_n = 13-17$  MeV, the measurement results for  $\sigma_f^7$  strongly diverge [8].

It is noteworthy that the data fall into two groups: those for absolute measurements of  $\sigma_f^7$ , and the data for relative (to the  $^{235}\text{U}$  fission cross-section) measurements. Rendering absolute the fission cross-section ratios by the threshold cross-section method (nuclide mixtures) to a considerable extent frees the relative values from the effects of target properties and the fragment recording efficiency associated therewith. This cannot be said for the results of absolute measurements.

$^{243}\text{Am}$  fission cross-section. Throughout almost the whole of the neutron energy range investigated, a systematic divergence is observed in the results of the measurements for  $\sigma_f(^{243}\text{Am})/\sigma_f(^{235}\text{U})$ . Again there are two sets of data differing in absolute value by 20% [9]. The cause of the divergence possibly lies in the extent to which the "absolutization" procedure  $\sigma_f^3/\sigma_f^5$  is correct. In the first group of studies use was made of threshold cross-sections and the data mutually coincide within the limits of error (2.5%). The data in the second group are derived by other methods and are considerably more strongly subject to the effects of the properties of the targets, primarily americium, which possesses substantial radioactivity. In no study are there any citations of experimental investigations on the values of the t/R of targets, and in the situation which has arisen it is precisely

the heightened (in comparison with calculations) value of  $t/R$  which could be the source of the divergences in question (the relevant parameters of the samples used for the studies in the second group were practically identical).

Targets as neutron sources. One of the important characteristics is the distribution of tritium through the thickness of a metallic target. As a rule, this ratio is not studied, although it may exercise an appreciable effect on experimental results.

The method of measuring the tritium concentration over the thickness (proposed by A.M. Davletshin and co-workers) is based on a comparison of the neutron yield from the target under investigation and a standard target of significantly less thickness. The measurements made at various incident particle energies lie within the limits of the energy width of the target ( $E_0 - \Delta E < E_i < E_0$ ), where  $i = 0, \dots, k$ . The neutron yield corresponding to energy  $E_m$ , is

$$Y_m = \sum_{i=0}^m C_i y_i, \quad m \leq k, \quad (3)$$

where  $C_i$  is the tritium concentration in the layer  $i$  in relation to the standard, and  $y_i$  is the yield from the standard target at energy  $E_i$ . The system of linear equations (3) has a stable solution. The accuracy of the method is not more than 7%. Investigation shows that the tritium distributions are frequently non-uniform. Targets are found with a double-humped distribution function, having its maximum near the boundary of the layer.

In a neutron source based on a gaseous target, a decisive part in the shaping of the neutron spectrum is played by the inlet window, made from fine metallic foil. For correct determination of the mean neutron energy and its dispersion it is necessary to measure the thickness of the window and the non-homogeneity of the foil surface. Both these quantities can be measured with good accuracy by reference to the transmission of  $\alpha$ -particles from radioactive sources [10]. The width of the  $\alpha$ -peak beyond the foil is used

to determine the energy spread  $\sigma_e$  associated with the inhomogeneity of the foil  $\sigma_R$ :

$$\sigma_E^2 = \left\{ \left[ \frac{dE}{dx}(E_0) \right]^2 + \left[ \frac{dE}{dx}(E_1) \right]^2 \right\} \sigma_R^2 .$$

Measurements with various foils [10] showed that the quantity  $\sigma_R$  can vary considerably.

#### REFERENCES

- [1] MALINOVSKIY, V.V., VOROB'EVA V.G., KUZ'MINOV, B.D. et al., At. Ehnerg. 56 (1983) 51 (in Russian).
- [2] KORNILOV, N.V., BARYBA, V.Ya., In: Neutron Physics, Proceedings of the 5th All-Union Conference on Neutron Physics, Kiev, 15-19 September 1980: Moscow, TsNIIatominform (1980) Part 3, 104, (in Russian).
- [3] BEHRENS, J.W., CARLSON, G.W., Nucl. Sci. and Engng., 63 (1977) 250.
- [4] GOVERDOVSKIY, A.A., GORDYNSHIN, A.K., KUZ'MINOV, B.D. et al., Vopr. atom. nauk. i tekhn. Ser. Yad. Konst. 3 (57) (1984) 13 (in Russian).
- [5] CARLSON, G.W., Nucl. Instrum. and Methods, 119 (1974) 97.
- [6] BUDTZ-JOERGENSEN, C., KNITTER, H.H., Proc. Intern. IAEA meeting 1984. Vienna: IAEA, TECDOC-335 (1985) 476.
- [7] VOROB'EVA, V.G., D'YACHENKO, P.P., KUZ'MINOV, B.D., TARASKO, M.Z., Yad. Fiz. 4 (2) (1966) 325 (in Russian).
- [8] IGNATYUK, A.B., Proc. Intern. symposium on nuclear physics, nuclear fusion, Nov. (1985) Gaussig: Zfk (1986) 112.
- [9] FURSOV, B.I., SAMYLIN, B.F., SMIRENKIN, G.N. et al., At. Ehnerg. 59 (1985) 339.
- [10] KORNILOV, N.V., Proc. Intern. IAEA meeting on neutron source properties. Leningrad, 1986.

Paper received by editors on 29 October 1987.



CROSS-SECTIONS FOR THE PRODUCTION OF  $\gamma$ -RAYS BY THE INTERACTION  
OF 3.0 MeV NEUTRONS WITH  $^{232}\text{Th}$ ,  $^{235}\text{U}$  and  $^{238}\text{U}$  NUCLEI

A.A. Filatenkov, M.V. Blinov, S.V. Chubaev, V.M. Saidgareev

CROSS-SECTIONS FOR PRODUCTION OF  $\gamma$ -RAYS BY INTERACTION OF 3.0 MeV NEUTRONS WITH  $^{232}\text{Th}$ ,  $^{235}\text{U}$  AND  $^{238}\text{U}$  NUCLEI. Spectra and total cross-sections of  $\gamma$ -rays produced in the energy range 0.25-3.55 MeV by 3.0 MeV neutrons were measured. Substantial disagreement with the BNAB-78 evaluation was revealed. A large number of monochromatic  $\gamma$ -transitions were observed. About 20  $\gamma$ -transitions are assigned to fission fragment prompt  $\gamma$ -rays.

The  $\gamma$ -radiation occurring upon interaction of fast neutrons with fissionable nuclei has a complex nature. In addition to a large number of discrete  $\gamma$ -transitions, it contains an intense continuous component. For a number of practical operations, such as calculation of nuclear reactor shielding and core heating, it is necessary to know the total spectrum. In the present work we measure the spectra and total cross-sections for formation of  $\gamma$ -photons in the energy range 0.25-3.55 MeV, at an incident neutron energy of 3.0 MeV and for the nuclides  $^{235}\text{U}$ ,  $^{238}\text{U}$  and  $^{232}\text{Th}$ . The measurements were carried out on an NG-400 neutron generator, operating in pulsed mode. The  $\gamma$ -radiation was recorded in a time window (20 ns) by a Ge(Li) detector. The following metallic samples were used: a  $^{238}\text{U}$  sheet, 35 mm long, 27 mm wide and 1.5 mm thick; a  $^{238}\text{U}$  cylinder of diameter 21.7 mm and height 27.0 mm; a  $^{232}\text{Th}$  cylinder of diameter 21.7 mm and height 27.0 mm; and a  $^{235}\text{U}$  cylinder of diameter 15.5 mm and height 28.1 mm.

The measurement method was perfected by comparison with that described in Ref. [1]. For further reduction of the background the detector shielding was strengthened somewhat, and a shadow cone made of borated polyethylene, 12 cm long, was introduced. The experiment was automated on the basis of a MERA-60 microcomputer operating on line [2]. One of the purposes of automation is to ensure stable operation of the experimental equipment over a considerable period of time (the total duration of the experiment was about 1000 hours). For this purpose, various parameters of the setup, including

those of the accelerator beam, were appropriately coded and inputted. During the collecting and sorting of the data, the control program continuously monitored the states of the setup.

The data were processed on MERA-60, SM-4, and ES-1033 computers. Processing included determination of the calibration parameters of the spectrometer using  $^{226}\text{Ra}$  and  $^{24}\text{Na}$  sources and an OSGI set, construction of the spectrometer response matrix, determination of the energy and intensity of discrete  $\gamma$ -transitions and subtraction of their contribution from the instrument (recorded) distribution, smoothing and restoration of the shape of the real  $\lambda$  spectrum using regularization methods [3], calculation by a Monte Carlo method of the neutron flux attenuation and  $\gamma$ -spectrum distortion in the sample, and other operations.

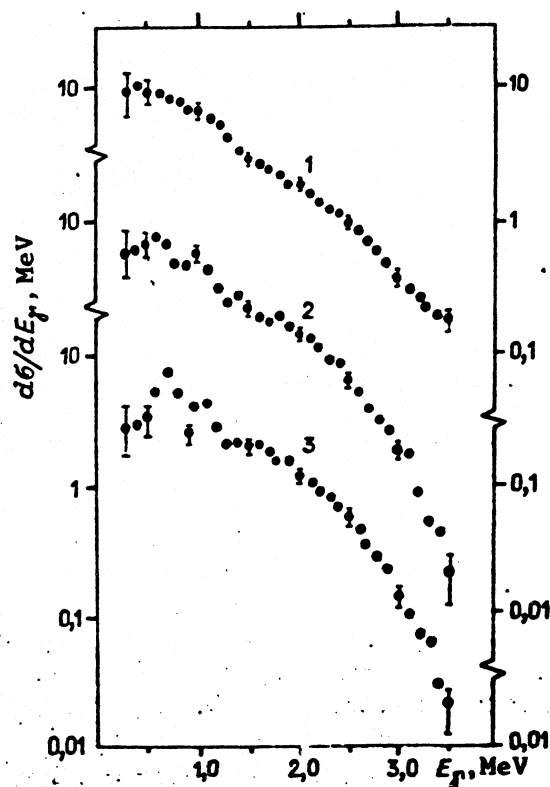
The validity of the corrections made for the effects of finite geometry in a thick sample was checked by comparison of the basic results obtained for a cylindrical  $^{238}\text{U}$  sample with the control results derived for a thin sheet of this nuclide. In the last case the corrections are not large and can be easily calculated analytically.

The overall error in determination of the  $\gamma$ -energy spectrum in our experiment amounted to 6-20%, its maximum being attained in the soft area of the spectrum, then smoothly sinking to its minimum value in the 1.5-1.7 MeV energy region, and again rising to 10-12% at the end of the energy range.

The cross-sections for the excitation of  $\gamma$ -transitions were determined with reference to a known cross-section for excitation of the 847 keV transition in the  $^{56}\text{Fe}(n,n',\gamma)$  reaction, which in accordance with the evaluation of the ENDL library was taken as 1020 mb for natural iron. The total cross-section for production of  $\gamma$ -photons was derived by multiplying the differential cross-section measured at an angle of  $125^\circ$  by  $4\pi$ .

The results are given in the figure. The spectra are broken down into groups each of 100 keV width. Under these conditions the discrete component of the spectrum for  $^{232}\text{Th}$  is still clearly discernible, it is somewhat less





Cross-sections for production of  $\gamma$ -rays by interaction of neutrons (3.0 MeV) with  $^{235}\text{U}$ ,  $^{238}\text{U}$  and  $^{232}\text{Th}$  nuclei (1, 2, 3 respectively).

visible for  $^{238}\text{U}$  and it is almost smoothed out for  $^{235}\text{U}$ . The total cross-section for formation of  $\gamma$ -rays in the energy range 0.25–3.55 MeV with de-excitation times of less than  $10^8$  s was  $(11.9 \pm 0.6)\text{b}$  for  $^{235}\text{U}$ ,  $(8.2 \pm 2.4)\text{b}$  for  $^{238}\text{U}$  and  $(6.1 \pm 0.2)\text{b}$  for  $^{232}\text{Th}$ . (The error in the value for the reference cross-section was not taken into account.)

A comparison was made between the results obtained with evaluated data available in the BNAB-78 library [4] for neutrons of the third group (2.5–4.0 MeV). The spectra measured were here broken down into groups corresponding to the BNAB format. The results of the comparison are contained in Table 1.

The comparison showed that the spectra as measured by the authors is harder. A particularly large divergence is observed for the group of  $\gamma$ -quanta with energies of 1.75–2.5 MeV, where the contribution of inelastic scattering gammas becomes substantial. In our opinion, the cause of this divergence lies in the fact that in the BNAB-78 evaluation the  $\gamma$ -ray

**Table 1.** Cross-sections for production of the  $\gamma$ -rays by interaction of 3.0 MeV neutrons with  $^{235}\text{U}$  and  $^{238}\text{U}$  nuclei.

$\gamma$ -quantum energy, MeV	$^{235}\text{U}$		$^{238}\text{U}$	
	BNAB-78	Present work	BNAB-78	Present work
0,35-0,75	4,32	4,02 $\pm$ 0,37	3,21	2,88 $\pm$ 0,26
0,75-1,25	3,00	3,54 $\pm$ 0,14	2,18	2,33 $\pm$ 0,10
1,25-1,75	1,34	1,68 $\pm$ 0,06	0,99	1,14 $\pm$ 0,04
1,75-2,50	0,85	1,28 $\pm$ 0,04	0,54	0,97 $\pm$ 0,03
2,50-3,50	0,41	0,47 $\pm$ 0,02	0,22	0,23 $\pm$ 0,02

**Table 2.** Gamma-radiation yields (Y) of fragments from 3 MeV neutron fission of  $^{235}\text{U}$  and  $^{238}\text{U}$  ( $\tau < 10^{-8}$  s).

Nuclide	$I_i^{\pi} - I_f^{\pi}$ [9]	$^{235}\text{U}$		$^{238}\text{U}$		$^{235}\text{U} + n_{\text{therm.}}$ [10]		$^{235}\text{U} + n_{\text{therm.}}$ [8]
		$E_{\gamma}$ , keV	$Y_{\gamma}$ , %	$E_{\gamma}$ , keV	$Y_{\gamma}$ , %	$E_{\gamma}$ , keV	$Y_{\gamma}$ , rel. unit	$Y_{\text{frag}}$ , %
$^{84}\text{Se}$	$2^+_{\text{g}} - 0^+_{\text{g}}$	1454,1(4)	0,7(3)	1454,0(5)	0,8(3)	-	-	0,70
$^{87}\text{Br}$	-	468,3(4)	0,7(4)	468,3(3)	0,7(3)	-	-	1,27
$^{88}\text{Kr}$	$2^+_{\text{g}} - 0^+_{\text{g}}$	775,4(2)	1,5(3)	774,7(4)	1,0(3)	-	-	1,72
$^{90}\text{Kr}$	$2^+_{\text{g}} - 0^+_{\text{g}}$	706,9(1)	5,0(6)	706,9(1)	4,4(4)	706(4)	70(23)	4,49
	$2^+_{\text{f}} - 0^+_{\text{g}}$	1362,5(4)	1,1(2)	1362,0(5)	1,4(2)	-	-	-
	$2^+_{\text{f}} - 2^+_{\text{g}}$	654,6(3)	1,1(3)	654,7(4)	1,1(3)	-	-	-
$^{92}\text{Sr}$	$2^+_{\text{g}} - 0^+_{\text{g}}$	814,6(4) <sup>a</sup>	4,0(5) <sup>a</sup>	814,8(3) <sup>a</sup>	2,8(3) <sup>a</sup>	-	-	1,17
$^{94}\text{Sr}$	$2^+_{\text{g}} - 0^+_{\text{g}}$	837,1(2)	3,8(5)	836,9(3)	2,6(3)	834(4)	61(20)	4,56
$^{95}\text{Sr}$	-	352,0(1) <sup>b</sup>	5,8(7) <sup>b</sup>	352,2(1) <sup>b</sup>	7,1(7) <sup>b</sup>	-	-	4,38
$^{96}\text{Sr}$	$2^+_{\text{g}} - 0^+_{\text{g}}$	814,6(4) <sup>a</sup>	4,0(5) <sup>a</sup>	814,8(3) <sup>a</sup>	2,8(3) <sup>a</sup>	813(4)	80(27)	3,54
$^{98}\text{Zr}$	$2^+_{\text{g}} - 0^+_{\text{g}}$	1223,6(4)	2,3(4)	1223,2(4)	2,5(5)	1224(5)	29(15)	2,67
$^{100}\text{Zr}$	$2^+_{\text{g}} - 0^+_{\text{g}}$	-	-	212,5(4) <sup>z</sup>	5,0(9) <sup>z</sup>	212(2)	37(13)	4,56
	$4^+_{\text{g}} - 2^+_{\text{g}}$	352,0(1) <sup>b</sup>	5,8(7) <sup>b</sup>	352,2(1) <sup>b</sup>	7,1(7) <sup>b</sup>	351(3)	56(28)	-
	$6^+_{\text{g}} - 4^+_{\text{g}}$	497,6(2)	1,3(3)	497,3(3)	2,0(4)	495(3)	55(18)	-
$^{102}\text{Mo}$	$2^+_{\text{g}} - 0^+_{\text{g}}$	296,2(2) <sup>c</sup>	3,1(5) <sup>c</sup>	296,6(3) <sup>c</sup>	2,8(5) <sup>c</sup>	296(2)	9(3)	0,76
$^{134}\text{Te}$	$2^+_{\text{g}} - 0^+_{\text{g}}$	1279,8(4)	1,5(4)	1278,8(5)	2,6(3)	1278(5)	34(17)	6,78
	$4^+_{\text{g}} - 2^+_{\text{g}}$	296,2(2) <sup>c</sup>	3,1(5) <sup>c</sup>	296,6(3) <sup>c</sup>	2,8(5) <sup>c</sup>	-	-	-
$^{138}\text{Xe}$	$2^+_{\text{g}} - 0^+_{\text{g}}$	588,9(2)	4,7(6)	589,2(2)	2,3(5)	585(4)	106(60)	5,03
	$4^+_{\text{g}} - 2^+_{\text{g}}$	482,2(2)	4,6(6)	482,6(3)	2,2(6)	482(3)	112(37)	-
$^{140}\text{Xe}$	$2^+_{\text{g}} - 0^+_{\text{g}}$	376,1(3)	2,2(4)	376,6(2)	4,9(6)	373(3)	70(35)	3,88
	$4^+_{\text{g}} - 2^+_{\text{g}}$	456,9(3)	2,5(5)	457,6(2)	4,9(6)	-	-	-
$^{142}\text{Ba}$	$2^+_{\text{g}} - 0^+_{\text{g}}$	359,8(3)	2,6(6)	359,0(3)	1,9(5)	357(3)	35(12)	2,72

spectrum for the (n,n'γ) reaction is not quite correctly determined. Thus, the mean energy transferred by γ-quanta in one inelastic scattering event amounts, according to the evaluation, to 1.31 MeV for  $^{235}\text{U}$  and 1.86 MeV for  $^{238}\text{U}$ , although the law of conservation of energy requires that  $\bar{E}_{\gamma} = \bar{E}_n - \bar{E}_{n'} \approx 2.3 \text{ MeV}$ . The data from our experiments are in better correlation with the expected values.

Unfortunately, it was impossible to conduct a direct comparison of our results with those of other experiments carried out under similar conditions (i.e. with time selection of γ-quanta at 3.0 MeV neutron energy) in view of the absence of such material in the literature. The data in Ref. [5] on cross-sections for formation of γ-radiation upon interaction of  $^{235}\text{U}$  with 2 MeV neutrons are in reasonable agreement with the present figures. The results of the statistical calculation carried out for  $^{238}\text{U}$  in Ref. [6] are also nearer to our data than is the BNAB-78 evaluation.

From our previous publications [1, 7] devoted to investigation of the discrete part of the γ-spectrum for the nuclides in question, it emerged that fission fragment γ-radiation may be present among the γ-transitions detected in these studies. Using the results of our latest measurements in conjunction with those earlier obtained, also introducing data on the mass distribution of fission fragments [8] and on their level schemes [9], and furthermore having recourse to other studies [10-12], we succeeded in identifying about 20 γ-transitions in the  $^{235}\text{U}$  and  $^{238}\text{U}$  spectra, which relate to fission fragment prompt γ-radiation.

The experimental values for the energies of these γ-transitions and their yield for fission event are shown in Fig. 2. The experimental error in units of the last sign is given in brackets. An asterik marks those γ-transitions coinciding in terms of energy with one of the transitions of the (n,n'γ) reaction. If two close γ-radiation energies have two different fragments, such cases are indicated by a letter.

A certain pattern emerges from the results obtained. Thus, it will be noted that the  $\gamma$ -radiation yield of the nuclides in the left wing of the light peak (krypton and strontium) are somewhat greater on  $^{235}\text{U}$  fission than on  $^{238}\text{U}$  fission, reflecting the corresponding shift in the position of the light peak. Worthy of note also is the correlated change in the yields of transitions  $4_g^+ - 2_g^+$  and  $2_g^+ - 0_g^+$  in the nuclides  $^{138}\text{Xe}$  and  $^{140}\text{Xe}$ , which may be regarded as the result of development of a different structure in the heavy peak on  $^{235}\text{U}$  and  $^{238}\text{U}$  fission. However, on average the  $\gamma$ -transition yields  $2_g^+ - 0_g^+$  are close to the independent fragment yields measured for the case of thermal neutron fission of  $^{235}\text{U}$  [8].

Table 2 also shows the data from Ref. [9] in which the  $\gamma$ -radiation occurring on thermal neutron fission of  $^{235}\text{U}$  is recorded in fragment coincidences. The reliability of identification of  $\gamma$ -transitions in such an experiment is high, but the accuracy of determination of energies and areas of the  $\gamma$ -peak, when using thin targets is low, owing to the Doppler broadening of the lines and their weak intensity.

In the present experiment, as was stated above, we used fairly massive samples, which did not permit selection of fission event and fragment mass. However, in this case the accuracy of determination of the energies and intensities of  $\gamma$ -transitions is considerably greater and, we believe, the data given in Table 2 indicate the potentialities of the method for studying induced nuclear fission reactions.

The principal results of our work may be summarized as follows:

1. The energy spectra and total cross-sections for formation of  $\gamma$ -radiation in the 0.25-3.55 MeV energy range at incident neutron energy 3.0 MeV were measured for the  $^{235}\text{U}$ ,  $^{238}\text{U}$  and  $^{232}\text{Th}$  nuclei;
2. A comparison was made between the total spectra and cross-sections and available experimental data and the BNAB-78 evaluation. It emerged that in the 1.0-2.5 MeV  $\gamma$ -energy region, the data of the

experiment exceed the BNAB-78 evaluation by a factor of 1.2-1.8.

This divergence would appear to originate from failure to take adequate account, in the evaluation, of the contribution of  $\gamma$ -radiation from the  $(n,n'\gamma)$  reaction;

3. In the  $^{235}\text{U}$  and  $^{238}\text{U}$  spectra we identified about 20  $\gamma$ -transitions associated with fission fragment prompt  $\gamma$ -radiation ( $\tau < 10^{-8}\text{s}$ ), and determined their energies, place in the level scheme and yields per fission event;
4. An indication of the different fine structure of the heavy peak on 3.0 MeV neutron fission of  $^{235}\text{U}$  and  $^{238}\text{U}$  (yields of nuclides  $^{138}\text{Xe}$  and  $^{140}\text{Xe}$ ) was detected.

#### REFERENCES

- [1] BLINOV, M.V., STSIBORSKIY, B.D., FILATENKOV, A.A., SHIRYAEV, B.M., Gamma-radiation spectra occurring on interaction of 3 MeV neutrons with  $^{232}\text{Th}$ ,  $^{235}\text{U}$  and  $^{238}\text{U}$  nuclei. Vopr. atom. nauk. i tekhn. Ser. Yad. Konst. 3 (57) (1984) (in Russian).
- [2] SAIDGAREEV, V.M., FILATENKOV, A.A., CHUBAEV, S.V., Automated gamma-spectrometer with time channel for use on accelerator beam. Abstracts of the XXXVI meeting on nuclear spectroscopy and the structure of the atomic nucleus, Leningrad, Nauka (1986) 404 (in Russian).
- [3] TIKHONOV, A.N., ARSENIN, V.Ya., in: Methods of solving incorrect problems. Moscow, Nauka (1979) (in Russian).
- [4] ABAGYAN, L.P., BAZAZYANTS, N.O., NIKOLAEV, M.N., TSIBULYA, A.M., in: Group constants for reactor and shielding calculations. Moscow, Energoizdat (1981) (in Russian).
- [5] DRAKE, D.M., Cross-sections of uranium-235 and plutonium-239 for neutron producing  $\gamma$ -rays. Nucl. Sci. Engng., 55 (1974) 427-439.
- [6] TAKAHASHI, H., Gamma-ray production cross-sections of neutron-induced uranium-238 reactions. Ibid. 51 (1973) 269-315.
- [7] KOZULIN, E.M., TUTIN, G.A., FILATENKOV, A.A., Gamma-radiation spectrum occurring on interaction of 3 MeV neutrons with  $^{238}\text{U}$  nuclei. In: Neutron physics: Proceedings of the 5th All-Union conference on neutron physics, Kiev 15-19 September 1980. Moscow, TsNIIatominform (1980), Part 2, 25-29 (in Russian).
- [8] GANGRSKIY, Yu.P., DALKHSUREN, B., MARKOV, B.N., Nuclear fission fragments, Moscow, Energoizdat (1986) (in Russian).

- [9] SAKAI, M., Quasi-bands in even-even nuclei. Atomic Data and Nucl. Data Tables, 31 (1984) 399-433.
- [10] KHAN, T.A., HOFMAN, D., HORSCH, F., A study of the de-excitation of primary fission fragments from the neutron-induced fission of  $^{235}\text{U}$ . Nucl. Phys. A205 (1973) 488-512.
- [11] LEDERER, M.C., SCHIRLEG, V., Tables of isotopes. Seventh edition, New York, 1978.
- [12] JOHN, W., GUY, F.W., WESOŁOWSKY, J.J., Four-parameter measurements of isomeric transitions in  $^{252}\text{Cf}$  fission fragments. Phys. Ref., C2 (1970) 1451.

Paper received by editors on 23 July 1987.